

An-Najah National University
Faculty of Graduate Studies

**Design of A Fault-Tolerant Active Power Filter With
Active and Reactive Power Injection Capability Using
Multi-Level Inverter and Photovoltaic Array**

By
Amin Madi

Supervisor
Dr. Kamel Saleh

**This Thesis is Submitted in Partial Fulfillment of the Requirements for
the Degree of Master of Electrical Power Engineering, Faculty of
Graduate Studies, An-Najah National University, Nablus - Palestine.**

2018

**Design of A Fault-Tolerant Active Power Filter With
Active and Reactive Power Injection Capability Using
Multi-Level Inverter and Photovoltaic Array**

**By
Amin Madi**

This Thesis was defended successfully on 13/5/2018 and approved by:

Defense Committee Members

Signature

- Dr. Kamel Saleh	/ Supervisor
- Dr. Jaser Sa'ed	/ External Examiner
- Prof. Marwan Mahmoud	/ Internal Examiner

Dedication

To my father

To my mother, brothers and sisters

To my wife Eman

To my son Omar

To my daughter Shahd

To all friends and colleagues

To my teachers.

To all of them,

I dedicate this work.

Acknowledgments

It is an honor for me to have the opportunity to thank my Supervisor, Dr. Kamel Saleh for his valuable suggestions and encouragement. This work would not have been possible without his support and guidance. My appreciations go to staff of electrical power engineering Master Program especially

Prof. Marwan Mahmoud for his efforts to improve my knowledge.

My thanks go also to my small family, my kids Omar and Shahd and my wife for here encouragement and patience.

الإقرار

أنا الموقع أدناه مقدمة الرسالة التي تحمل العنوان:

Design of A Fault-Tolerant Active Power Filter With Active and Reactive Power Injection Capability Using Multi-Level Inverter and Photovoltaic Array

أقر بأن ما اشتملت عليه هذه الرسالة هو نتاج جهدي الخاص، باستثناء ما تمت الإشارة إليه حيثما ورد، وأن هذه الرسالة ككل أو أي جزء منها لم يقدم من قبل لنيل أي درجة أو لقب علمي أو بحثي لدى أي مؤسسة تعليمية أو بحثية أخرى.

Declaration

The work provided in this thesis, unless otherwise referenced, is the researcher's own work, and not been submitted elsewhere for any other degrees or qualifications.

Student's name:

اسم الطالب:

Signature:

التوقيع:

Date:

التاريخ:

Table of Contents

No	Content	Page
	Dedication	iii
	Acknowledgment	iv
	Declaration	v
	Table of Figures	ix
	List of Abbreviations	xiii
	Abstract	xiv
	Chapter One: Introduction	1
1.1	Background	1
1.2	Harmonic Mitigation Techniques	2
1.3	Motivation	3
1.3.1	Power System Quality	3
1.3.2	Reliability of Filter	8
1.4	Objectives	8
1.5	Thesis Structure	9
	Chapter Two: Parallel Active Filter	11
2.1	Introduction	11
2.2	Harmonic Currents Extraction Methods	13
2.2.1	Instantaneous Active and Reactive Power Theory	13
2.2.1.1	Introduction	13
2.2.1.2	Instantaneous Active and Reactive Power (p-q) Calculation	14
2.2.2	Instantaneous Active and Reactive Current Component (id-iq) Method	50
2.3	Control of the Active Power Filter	22
2.3.1	Direct Control Method	23
2.3.1.1	Control in the Three Phase Reference	25
2.3.1.2	Control in the Synchronous Frame Reference d-q	26
2.3.2	Indirect Control of the Active Power Filter	26
2.3.2.1	Grid Current Reference Generation	27
2.3.2.1.1	PQ Theory Based Algorithm	27
2.3.2.1.2	Synchronous Reference Based Method	29
2.3.2.2	Design of SHAPF Controller	30
	Chapter Three: Grid Connected PV System With MPPT	41
3.1	Introduction	41
3.2	Photovoltaic Arrangements	41
3.2.1	PV Cell	41
3.2.2	PV Model	42
3.2.3	Photovoltaic Array	43

3.3	Modeling of PV Array	43
3.4	PV Array Characteristic Curves	47
3.4.1	Current Versus Voltage and Power Versus Voltage Curves	47
3.4.2	Effect of Changing Temperature on Characteristic Curves	48
3.4.3	Effect of Changing Temperature on Characteristic Curves	49
3.5	Maximum Power Point Tracking (MPPT)	50
3.6	Perturb and Observe (P&O) MPPT	51
3.6.1	Basic Concept	51
3.6.2	Flow Chart of (P&O) Algorithm	52
3.7	Boost Converter	53
3.7.1	The Operation of Boost Converter	55
3.7.1.1	Charging Mode of Operation	55
3.7.1.2	Mode-2 or Discharging Mode of Operation	56
3.7.2	Waveforms	57
3.8	Design of the System (PV and Boost Converter)	57
3.8.1	Design of the PV System	57
3.8.2	Calculation of Boost Converter Parameters	60
	Chapter Four: Multilevel Inverter	64
4.1	Introduction	64
4.2	Multilevel Converter Structures	65
4.2.1	Diode-Clamped Multilevel Inverter	66
4.2.1.1	Advantages and Disadvantages of DCMLI	68
4.2.2	Flying Capacitor Multilevel Inverter	68
4.2.2.1	Advantages and Disadvantages of (FCMLI)	69
4.2.3	Cascaded Multilevel Inverter	70
4.2.3.1	Operation of CMLI	71
4.2.3.2	Advantages and Disadvantages of CMLI	72
4.3	Multilevel Inverter Design	72
4.4	Results	78
4.4.1	Simulation of Tow-Level Inverter with Sinusoidal Input	79
4.4.2	Simulation of Nine-Level Cascade Inverter with Sinusoidal Input	80
4.4.3	Simulation of 27 Level Cascade Inverter with Sinusoidal Input	80
4.4.4	Simulation of Three Levels Inverter	81
4.4.5	Simulation of 27 Level Inverter	82

	Chapter Five: Fault Tolerant Techniques For The H-Bridge Inverter	84
5.1	Introduction	84
5.2	Fault-Tolerant Two-Level Inverter Techniques	86
5.3	Fault-Tolerant Multilevel Inverters	90
5.4	Control Strategy for the Open Circuit Fault Adopted in the Project	92
	Conclusions	96
	References	98
	المخلص	ب

Table of Figures

No	Figures	Pages
Figure (1.1)	Shunt passive high pass filter	4
Figure (1.2)	Shunt active power filter scheme	5
Figure (1.3)	Hybrid power filter scheme	6
Figure (2.1)	Current source active filter (CSAF) circuit	12
Figure (2.2)	Voltage source active filter (VSAF) circuit	12
Figure (2.3)	a-b-c to the 0- α - β system	15
Figure (2.4)	Power components of the p-q theory in <i>a-b-c</i> coordinate	17
Figure (2.5)	Diagram of the p-q theory to eliminate harmonics	19
Figure (2.6)	Diagram of the p-q theory to eliminate harmonics and improving PF	20
Figure (2.7)	Reference current extraction with <i>id-iq</i> method	22
Figure (2.8)	Direct control method	23
Figure (2.9)	Structure of current control loop	24
Figure (2.10)	Direct control method of SHAPF	24
Figure (2.11)	PI current controller loop	25
Figure (2.12)	Direct control using PI controllers in synchronous reference	26
Figure (2.13)	Diagram of indirect method control	27
Figure (2.14)	Indirect control based on the instantaneous power theory	29
Figure (2.15)	Diagram of indirect control based on the synchronous frame method	31
Figure (2.16)	Schematic of SAF	32
Figure (2.17)	Current controller	33
Figure (2.18)	Control strategy for the inverter	34

Figure (2.19)	Matlab simulink for (SHAPF) controller	34
Figure (2.20)	Matlab simulink for the designed system	36
Figure (2.21)	Output source current before and after filtering	36
Figure (2.22)	Spectrum of source current before and after filtering	37
Figure (2.23)	Waveform of the voltage and current of the source	37
Figure (2.24)	Focusing on the crossing point for both cases	38
Figure (2.25)	Power factor and reactive power produced by source	38
Figure (2.26)	Output source current during 3 stages	39
Figure (3.1)	PV cell structure	42
Figure (3.2)	Photovoltaic system	43
Figure (3.3)	Equivalent circuit PV cell	44
Figure (3.4)	Current versus voltage curve	48
Figure (3.5)	Power versus voltage curve	48
Figure (3.6)	Effect of changing solar irradiation	49
Figure (3.7)	V-I curves for many values of temperature	50
Figure (3.8)	V-P curves for many values of temperature	50
Figure (3.9)	Flow chart of (P&O) algorithms	52
Figure (3.10)	Boost converter	54
Figure (3.11)	Charging mode	56
Figure (3.12)	discharging mode of operation	56
Figure (3.13)	Waveforms of boost converter modes	57
Figure (3.14)	The configuration of PV generator	60
Figure (3.15)	Output voltage of the PV system	63
Figure (4.1)	One phase leg inverter with (a) two levels, (b) three levels, and (c) n levels	66

Figure (4.2)	Three level inverter using diode-clamped inverter topology	67
Figure (4.3)	Circuit topology for capacitor-clamped multilevel inverter (three levels)	69
Figure (4.4)	Three-level cascaded multilevel inverter (Y-configuration)	71
Figure (4.5)	27 level H-bridge inverter with three separate dc source	73
Figure (4.6)	Amplitude modulation flow chart	74
Figure (4.7)	The DC voltages arrangement for level 1	76
Figure (4.8)	The DC voltages arrangement for level 8	77
Figure (4.9)	The output voltages of each cell when (001110101110) produced	77
Figure (4.10)	27 level H-bridge inverter with its controller	78
Figure (4.11)	The input and output voltage signals using two level inverter	79
Figure (4.12)	The input and output signal using nine level h-bridge inverter	80
Figure (4.13)	The input and output signal using 27 level h-bridge inverter	81
Figure (4.14)	Output source current after using three level inverter	82
Figure(4.15)	Output source current before and after using 27 level inverter	83
Figure (5.1)	Diagram of the system with open circuit fault	85
Figure (5.2)	Output source current during open circuit fault	85
Figure (5.3)	Two-level three-phase inverter with fourth leg for fault tolerance	86

Figure (5.4)	Fault-tolerant topology for two level four-leg inverter	88
Figure(5.5)	Fault-tolerant topology for two level four-leg neutral-point- connected inverter	88
Figure (5.6)	Leg A with isolation capability	89
Figure (5.7)	Module with bypass contactor	91
Figure (5.8)	Fault tolerant scheme for one leg open circuit	92
Figure (5.9)	Control strategy scheme for open circuit fault	93
Figure (5.10)	Output current after applying new control strategy for open circuit fault	94
Figure (5.11)	Output source current before and after applying new control topology for open circuit fault	95
Figure (5.12)	Output source current before, during and fault tolerant stages	95

List of Abbreviations

DC	Direct Current
AC	Alternative Current
PSH	Peak Sun Hour
STC	Standard Test Condition
PV	Photovoltaic
VSI	Voltage Source Inverters
CSI	Current Source Inverter
DSP	Digital Signal Processors
MPPT	Maximum Power Point Tracking
SHAPF	Shunt Active Power Filter
VSAF	Voltage Source Active Filter
CSAF	Current Source Active Filter
DCMLI	Diode Clamped Multilevel Inverter
CMI	Cascaded Multilevel Inverter
PL	Phase Loss
SE	Solar Energy
PCC	Point of Common Coupling
APF	Active Power Filter
HPF	High Pass Filter
LPF	Low Pass Filter
PLL	Phase Lock Loop
IGBT	Insulated-gate Bipolar Transistors
FPSC	Fundamental Phase-shift Compensation
Wp	Watt Peak

**Design of A Fault-Tolerant Active Power Filter With Active and
Reactive Power Injection Capability Using Multi-Level Inverter and
Photovoltaic Array**

By

Amin Madi

Supervisor

Dr. Kamel Saleh

Abstract

The increasing use of nonlinear loads leads to increase the harmonic pollution in the main power system. Harmonics cause many power quality problems such as voltage distortions at Point of Common Coupling (PCC), changing peak-value and RMS-value of line current which will cause addition losses, overloading and overheating, failure of some electrical equipments as transformers, capacitors, and motors, circuit breakers will trip frequently, and damage fuses. Moreover, harmonics may cause interfering with telecommunication lines; therefore, the power quality will be affected. This thesis suggests a solution for this power quality problem through designing multitask active power filter which have the ability to mitigate harmonics, inject reactive power, improve power factor, inject real power and tolerate open circuit fault. The filter was designed and tested using MATLAB software and the results show improving in power quality. The Total Harmonic Distortion (THD) decreased from 13.9% to 3.9% after activating the APF and the power factor becomes nearly 1.0. The APF was tested during open circuit fault (one leg disconnected) and the result was

acceptable because the THD decreased from 42% to 8.4% which mean that the filter has the ability to work under fault condition with minimum possible distortion.

Chapter One

Introduction

1.1. Background

The nonlinear loads are widely used in modern electrical systems which lead to increase the harmonic pollution in the main power system. Harmonic currents caused by using power electronic devices such as mobile chargers, converters, or any electrical device containing semiconductor affect the power quality and create non-sinusoidal currents from the AC source. Switching operation which is done by the power converters makes the discontinuity in the current which means increasing the harmonics in the system. These power electronic devices make pollution in the power system and cause power quality problems and affect sensitive loads [1].

Harmonics in the power system cause many problems such as voltage distortions at Point of Common Coupling (PCC), changing peak-value and RMS-value of line current which will cause additional losses, overloading and overheating, failure of some electrical equipments as transformers, capacitors, and motors, circuit breakers will trip frequently, and damage fuses. Moreover, harmonics may cause interfering with telecommunication lines. Therefore, the power quality will be affected [2].

Beside the problems caused by harmonic current, reactive power is another problem to power quality in the power system. Reactive current is not a useful power and doesn't do real work in the power system and will cause

overloading in the elements that passes through them and causing additional losses because the RMS value of the current will increase [3]. In order to improve the power quality delivered to the system, the harmonics and reactive power have to be canceled by using any type of electrical filters.

Many types of filter topologies are used to improve the power quality like passive, active, and hybrid [4]. In this project, a parallel active filter is used to improve the electric power quality. This active filter can do many jobs, such as mitigating harmonics, compensating reactive power, improving power factor (PF), injecting real power, and having a fault tolerant capability to make the system stable and continue to deliver the power to the load during fault condition (one phase open circuit fault).

1.2. Harmonic Mitigation Techniques

Harmonic pollution can be solved in two methods. The first method is to use suitable circuit topologies that can reduce or prevent the harmonic pollution to be created. An example of these applications is using transformer-less UPS systems using PWM rectifier topologies which will create low harmonics in the current. Therefore, a small amount of distortion may remain and in this case no need to use filtering equipments. The second method is by using power filtering equipments and this method uses techniques to reduce the total harmonic distortion (THD_I) which is defined in equation (1.1). These techniques can be classified in three categories:

1. Passive filters.
2. Active filters.
3. Hybrid filters.

$$THD_I = \frac{\sqrt{\sum_{n=2}^{\infty} I_n^2}}{I_1} \quad (1.1)$$

The traditional filter is used is the passive filtering technique as shown in figure (1.1). The principle of passive filter is compensating harmonics through low impedance connected parallel to the load which is called (parallel passive filter) or through blocking them using high series impedance connected in series which is called series passive filter [4]. A combination of shunt and series can be used in some cases depending on the nonlinear load used.

The designer of filters sometimes preferred to use passive filter due to their simplicity, high efficiency (for cretin frequency), and low cost [5].

Although passive filters have many advantages but they depend on the system parameters, a problem of resonance with the system impedance will appear when using passive filters and it can be used to filter a cretin harmonic frequency [5]. Therefore, active filters are used.

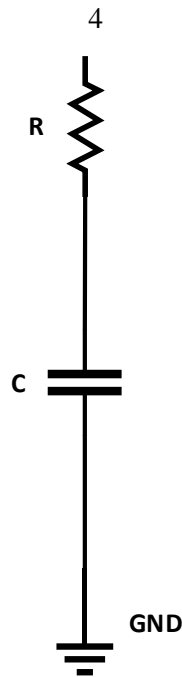


Figure (1.1): Shunt passive high pass filter (first order) [4].

The principle of the active filters was studied around 1970s. However, the idea becomes economically and technologically feasible when cost and fast semiconductor devices as MOSFETs, (IGBTs), and cost of high performance effective Digital Signal Processors (DSPs) became available. Moreover, the improvement in the control theory in power electronics helps the active filter to be practical and commercial success and become more efficient in filtering harmonics because the basic principle of the active filter is to inject voltage/current with same magnitude and opposite of the harmonics so harmonics will be eliminated from the system as shown in figure (1.2) [6].

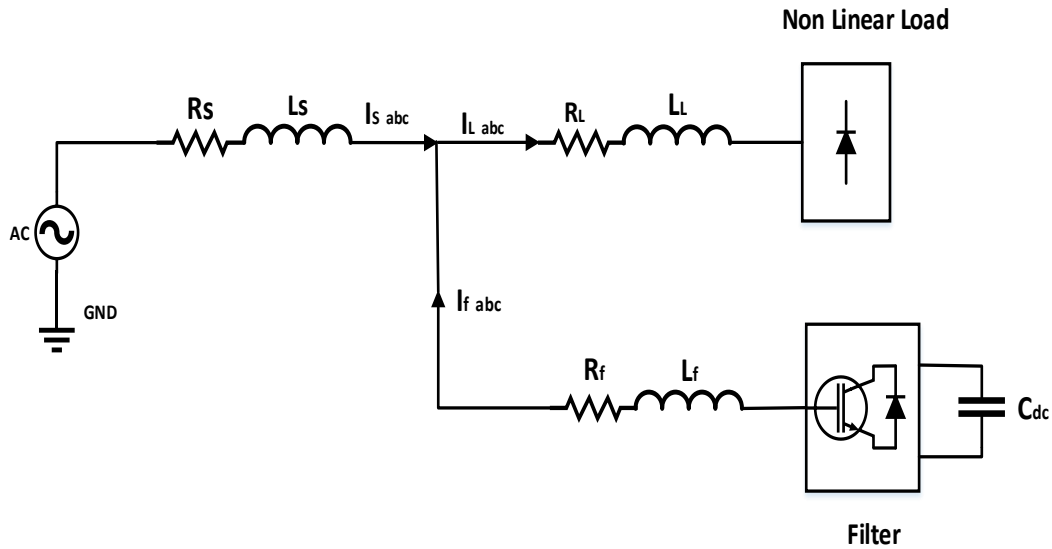


Figure (1.2): Shunt active power filter scheme.

Active filters have small physical size and can do many functions in the power system such as compensation reactive power, injecting real power and can tolerate faults and work properly under fault condition unlike passive filters. They act as effective solutions for many power quality problems. Although, active filters are effective in filtering, they need high cost compared to passive filters [6].

Active filters have some drawbacks as following:

- Requiring high converter ratings.
- Costlier when compared to passive filter.

Therefore, to avoid the disadvantages of passive and active filters, a new type of filters which is called hybrid power filter is used. Hybrid filters consist of two types of filters, the first one is active and the second one is passive or any two different types. Hybrid filters are used to reduce initial

cost and increase the efficiency of the system. The passive filter (used in hybrid) is used to eliminate high power and low order harmonics while the active filter is used to eliminate high order with low power harmonics [7].

The principle of hybrid filtering is to improve the filtering capacity of a passive filter and to damp series and parallel resonances with a small rated active filter. However, the functionalities of hybrid filters are limited compared to pure active filters and they involve higher engineering effort than passive filter design [8].

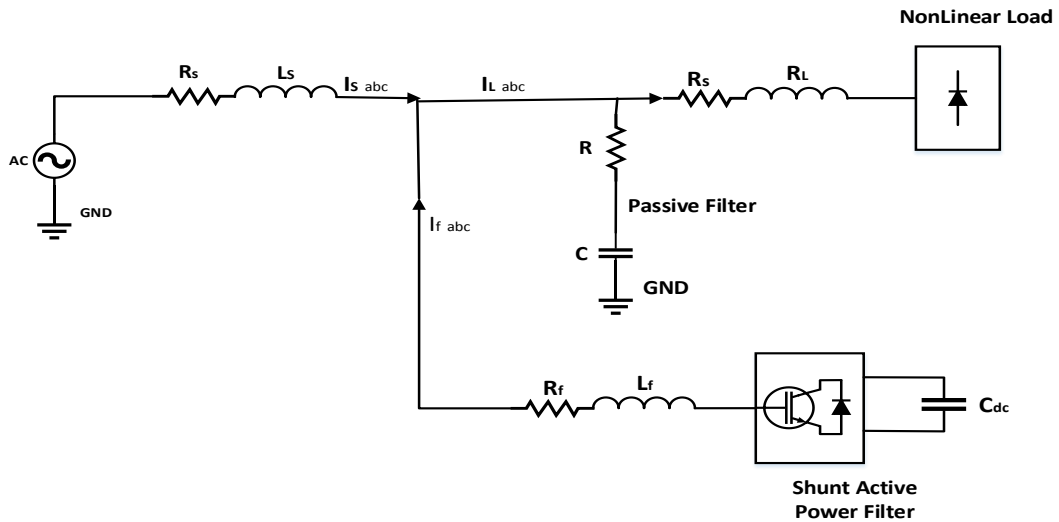


Figure (1.3): Hybrid power filter scheme.

1.3 Motivation

1.3.1 Power System Quality

The power quality is affected when there is any deviation in the voltage, current or frequency. The common problems that affect the sensitivity of the equipment are:

- Power Surges.
- Transients.
- Frequency Variation.
- Electrical Line Noise.
- Brownouts or Blackouts.
- Power System Faults.
- Improper grounding affect.
- Voltage sag.
- Voltage swells.

The main effect which is caused by most of these problems is the production of harmonics. The presence of harmonics deteriorates the quality of power and may damage the end user equipment.

Power system quality is an important issue in the power system for the above-mentioned reasons so, a suitable filter has to be designed to eliminate the harmonics, compensate the reactive power and improve the power factor (PF) to avoid problems that may appear in the power system.

1.3.2 Reliability of Filter

The filter should have the ability to work under a fault condition especially when one leg of the inverter is faulted. Because when the fault occurs, the filter becomes a source of pollution instead of solving the problems so, a filter with fault tolerant capability has to be designed.

1.4 Objectives

The objectives of this thesis are illustrated in the followings:

Design a fault-tolerant active power filter that has the capability to filter harmonics, compensate reactive power and inject real power to the grid which includes:

A- Design the four-leg inverter.

B- Choosing the type and the size of photovoltaic array needed in order to meet load reactive and real power demands.

C- Maximum power point tracker (MPPT) controller design.

A MPPT, or maximum power point tracker is an electronic DC to DC converter that optimizes and match between the solar array (PV panels), and the utility grid.

D- Fault tolerant capability for the inverter.

1.5 Thesis structure

1.5.1 Chapter one: Introduction

Chapter one talks about the effects of increasing use of nonlinear loads which cause harmonics in the power system and the effects of these harmonics on the grids and equipments. This chapter also reviews many methods to mitigate the harmonics and compensate the reactive power such as using power filters (passive, active and hybrid). Finally, it specifies the motivation and the objectives of this work.

1.5.2 Chapter two: Parallel Active Filter

Chapter two talks about Parallel Active Filter and its construction, operation and versus methods to extract the harmonics and it shows how to control the filter. Many methods reviewed in this chapter. Finally, the control circuit for the filter was designed and tested by using MATLAB software and the results were analyzed.

1.5.3 Chapter three: Grid Connected PV System with MPPT.

This chapter discusses how to make use of solar energy by using photovoltaic (PV) and the importance of using maximum power point tracking algorithms to get maximum possible power from the solar energy. This chapter also discusses the effects of the temperature and solar irradiation on the characteristic curves of the PV module. Boost converters operation and construction were also studied. Finally, a suitable design of

PV system with MPPT circuit were designed and tested and the results were discussed.

1.5.4 Chapter four: Multilevel Inverter.

This chapter discusses the different types of multilevel inverters and the advantages and disadvantages of each type. H-bridge multilevel inverter is chosen in the thesis, different levels of this type were designed and tested on the system and the results were compared.

1.5.5 Chapter five: Fault Tolerant Techniques for Multilevel Inverter.

Many faults tolerant techniques are reviewed in this chapter, and new fault technique is adopted which were used to control the motor speed in case of open circuit fault. This technique is tested on the inverter by assuming an open circuit fault happened and the result analyzed.

Chapter Two

Parallel Active Filter

2.1 Introduction

There are many types of power filters used in the power systems like series, parallel and hybrid power filters (a filter which consists of two types of filters to increase filtering efficiency). Series active filters are connected in series between loads and source, they are used to reduce and compensate load voltage harmonics. Parallel active filter also used to compensate current harmonics of the non linear loads.

A parallel active filter is chosen in this thesis to filter source current harmonics. It has lower component ratings than other types such as series active filters because the components in series filter should have the ability to pass total current throw it which means higher ratings for the components used [9].

There are two types of shunt active power filters (SHAPF); Voltage Source Active filter (VSAF) and Current Source Active filter (CSAF). The storage element used with these filters determines the type of the filter as shown in figures (2.1) and (2.2).

The basic concept of SHAPF is the ability to cancel harmonics by injecting equal but opposite harmonic current to the non-linear load. This mission can be achieved by using a suitable controller which drives switching elements (IGBTs) to produce reference signal.

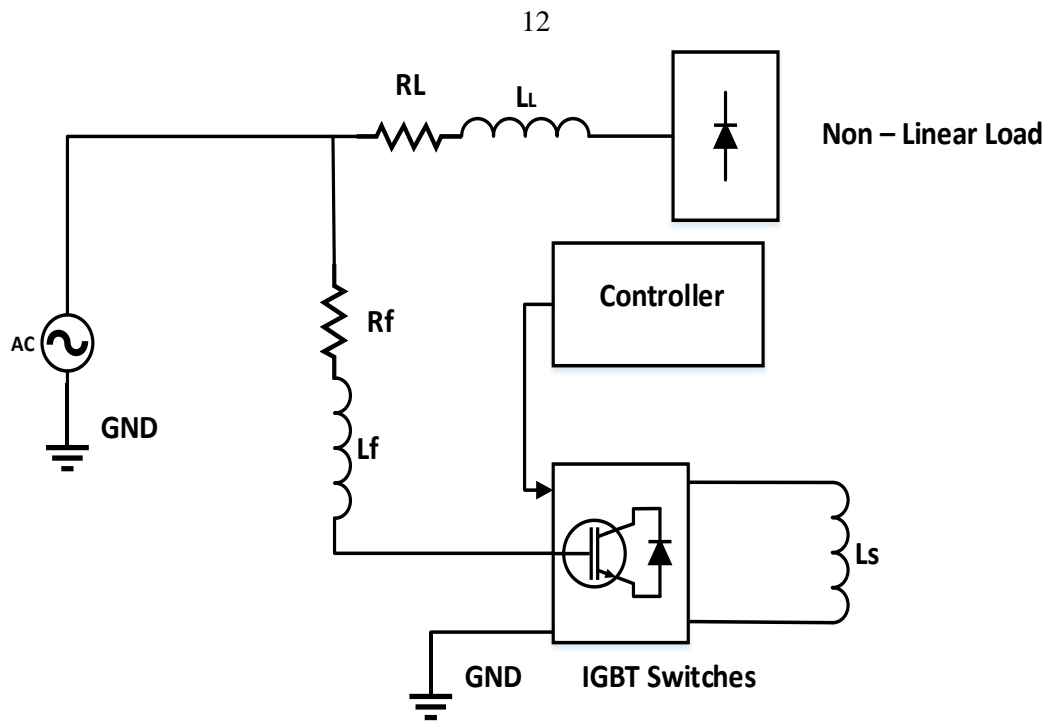


Figure (2.1): Current source active filter (CSAF) circuit.

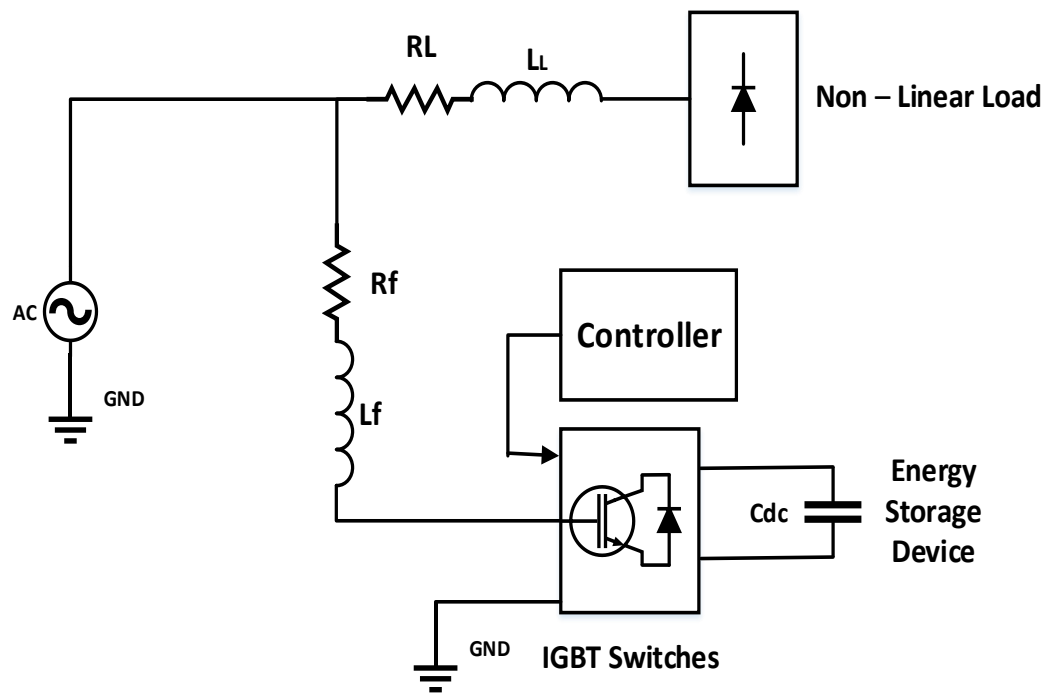


Figure (2.2): Voltage source active filter (VSAF) circuit.

VSAF is lighter, less expensive; fewer losses produced and simpler to control compared with the CSAF [10], so it is chosen in this project.

2.2 Harmonic Currents Extraction Methods.

The efficiency of the APF depends on the reference extraction method adopted. Many techniques are used to extract the reference signal. There are mainly two techniques, time domain and frequency domain [11]. In the time domain, an instantaneous estimation is done to generate reference signal from distorted load voltage or current. Time domain method simpler and need fewer calculation compared to frequency domain so the result will be faster[11].

2.2.1 Instantaneous Active and Reactive Power Theory.

2.2.1.1 Introduction

The p-q theory depends on the instantaneous power which is defined in time domain. This theory can be applied on three phase systems with both cases, with or without neutral wire. The first step in this theory is to transfer three phase current and voltage from a-b-c coordinates to Clarke or α - β -0 coordinates and calculate the instantaneous power using α - β -0 coordinates. Clarke transformation which consists of matrix that relate between three phase components and α - β -0 stationary reference frames is used [12]. Finally, reference current generated depending on active and reactive power of the non-linear load.

2.2.1.2 Instantaneous Active and Reactive Power (p-q) Calculation.

Akagi-Nabae proposed (p-q) theory which used to separate the fundamental and harmonic components of non-linear load power [13]. The three phase systems without zero sequence can be expressed as:

$$\mathbf{x}\mathbf{a} + \mathbf{x}\mathbf{b} + \mathbf{x}\mathbf{c} = \mathbf{0} \quad (2.1)$$

Equation (2.1) shows that there is only two variables because the third variable related (a function) to the two other variables.

A matrix as shown in equation (2.2) can be created to transform from a-b-c to α - β -0 system as shown below:

$$\begin{bmatrix} v_0 \\ v_\alpha \\ v_\beta \end{bmatrix} = \frac{\sqrt{2}}{\sqrt{3}} \begin{bmatrix} 1/\sqrt{2} & 1/\sqrt{2} & 1/\sqrt{2} \\ 1 & -1/2 & -1/2 \\ 0 & \sqrt{3}/2 & -\sqrt{3}/2 \end{bmatrix} \begin{bmatrix} v_a \\ v_b \\ v_c \end{bmatrix} \quad (2.2)$$

$$\begin{bmatrix} i_0 \\ i_\alpha \\ i_\beta \end{bmatrix} = \frac{\sqrt{2}}{\sqrt{3}} \begin{bmatrix} 1/\sqrt{2} & 1/\sqrt{2} & 1/\sqrt{2} \\ 1 & -1/2 & -1/2 \\ 0 & \sqrt{3}/2 & -\sqrt{3}/2 \end{bmatrix} \begin{bmatrix} i_a \\ i_b \\ i_c \end{bmatrix} \quad (2.3)$$

The theory depends on the transformation from the 3-phase system (a-b-c) to the 0- α - β system as shown in Figure (2.3).

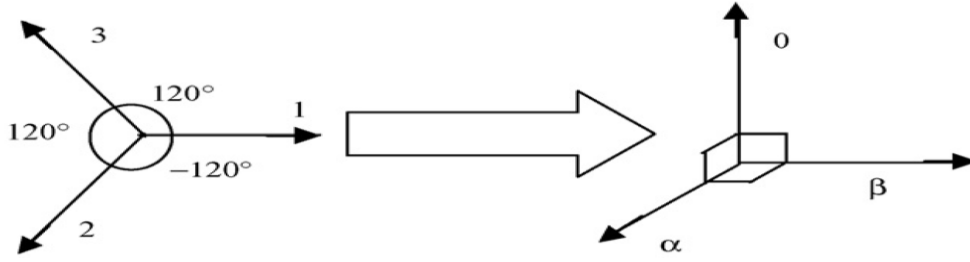


Figure (2.3): a-b-c to the 0-α-β system.

$$\begin{bmatrix} ia \\ ib \\ ic \end{bmatrix} = \frac{\sqrt{2}}{\sqrt{3}} \begin{bmatrix} 1/\sqrt{2} & 1 & 0 \\ 1/\sqrt{2} & -1/2 & \sqrt{3}/2 \\ 1/\sqrt{2} & -1/2 & -\sqrt{3}/2 \end{bmatrix} \begin{bmatrix} io \\ i\alpha \\ i\beta \end{bmatrix} \quad (2.4)$$

From equation (2.1) and (2.2) a new relation can be driven as following:

$$iN = ia + ib + ic = \sqrt{3} io \quad (2.5)$$

The power can be defined as following:

$$\begin{bmatrix} po \\ p\alpha\beta \\ q\alpha\beta \end{bmatrix} = \begin{bmatrix} vo & 0 & 0 \\ 0 & v\alpha & v\beta \\ 0 & -v\beta & v\alpha \end{bmatrix} \begin{bmatrix} io \\ i\alpha \\ i\beta \end{bmatrix} \quad (2.6)$$

Where va, vb, vc and ia, ib, ic are phase voltages and currents.

po -Is the zero sequence (real instantaneous power).

$p\alpha\beta$ -Is the instantaneous real power.

$q\alpha\beta$ -Is the instantaneous imaginary power.

Equation (2.3) can be rewritten by using power and voltages instead of currents as following:

$$\begin{bmatrix} io \\ i\alpha \\ i\beta \end{bmatrix} = \frac{1}{v_o(v\alpha\beta)^2} \begin{bmatrix} v\alpha\beta & 0 & 0 \\ 0 & vov\alpha & -vov\beta \\ 0 & vov\beta & vov\alpha \end{bmatrix} \begin{bmatrix} po \\ p\alpha\beta \\ q\alpha\beta \end{bmatrix} \quad (2.7)$$

$$\text{Where, } v\alpha\beta^2 = v\alpha^2 + v\beta^2 \quad (2.8)$$

There are six Power types in the p-q theory as following [12].

- $\overline{p0}$ - Instantaneous power which is transferred from source to the load through voltage and current (zero-sequence components).
- $\widetilde{p0}$ - Alternated value of instantaneous power which is exchanged between source and the load through zero-sequence components.
- \overline{p} - Instantaneous real power is transferred from the source to the load in a balanced way (power component which is desired).
- \widetilde{p} - Alternated value of the instantaneous real power is exchanged between the load and source and related to the harmonics.
- \overline{q} - The imaginary instantaneous power that belongs to the reactive power generated by the currents and voltages fundamental components.
- \widetilde{q} - The instantaneous imaginary power that belongs to the harmonic currents caused by the instantaneous reactive power AC component.

These power components are shown in the figure (2.4):

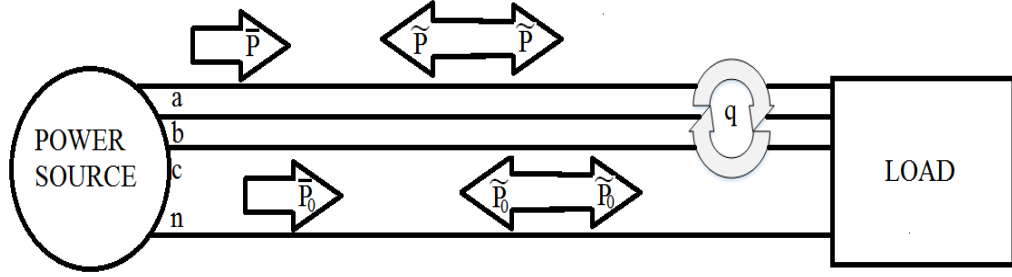


Figure (2.4): Power components of the p-q theory in *a-b-c* coordinate [12].

The only useful and desired power is \bar{p} component, so the active power filter has to compensate the other components to improve the power quality. If the neutral wire is not connected, the zero component voltage will be null value, and also null value for the zero current components. So equation (2.2) & (2.3) become as follows:

$$\begin{bmatrix} v\alpha \\ v\beta \end{bmatrix} = \frac{\sqrt{2}}{\sqrt{3}} \begin{bmatrix} 1 & -1/2 & -1/2 \\ 0 & \sqrt{3}/2 & -\sqrt{3}/2 \end{bmatrix} \begin{bmatrix} va \\ vb \\ vc \end{bmatrix} \quad (2.9)$$

$$\begin{bmatrix} i\alpha \\ i\beta \end{bmatrix} = \frac{\sqrt{2}}{\sqrt{3}} \begin{bmatrix} 1 & -1/2 & -1/2 \\ 0 & \sqrt{3}/2 & -\sqrt{3}/2 \end{bmatrix} \begin{bmatrix} ia \\ ib \\ ic \end{bmatrix} \quad (2.10)$$

The instantaneous power of the load (pl and ql) are given by the following equation:

$$\begin{bmatrix} pl \\ ql \end{bmatrix} = \begin{bmatrix} v\alpha & v\beta \\ v\beta & -v\alpha \end{bmatrix} \begin{bmatrix} i\alpha \\ i\beta \end{bmatrix} \quad (2.11)$$

Decomposing equation (2.11) gives the following:

$$pl = \widetilde{pl} + Pl \quad (2.12)$$

$$ql = \widetilde{ql} + Ql \quad (2.13)$$

Pl and Ql are average terms and \widetilde{ql} and \widetilde{pl} are oscillatory terms.

Many things can be noticed from the above equations. They are as follows:

- The average power represents the first harmonic (fundamental) current under sinusoidal and balanced condition [12].
- The oscillating terms related to all higher harmonics [12].

By using high pass filter (HPF) or low pass filter (depending on the design) as shown in figure (2.6), the average power terms can be eliminated, and the rest terms have to be compensated as follow:

$$pc = -\widetilde{pl} \quad \text{and} \quad qc = \widetilde{ql} \quad (2.14)$$

The current to be compensated as following:

$$\begin{bmatrix} ic\alpha \\ ic\beta \end{bmatrix} = \frac{1}{v\alpha v\beta^2} \begin{bmatrix} v\alpha & v\beta \\ v\beta & -v\alpha \end{bmatrix} \begin{bmatrix} pc \\ qc \end{bmatrix} \quad (2.15)$$

Where $v\alpha\beta^2 = v\alpha^2 + v\beta^2$.

By transforming between α - β coordinate to a-b-c coordinate the reference current which have to be generated by the inverter becomes:

$$\begin{bmatrix} ica^* \\ icb^* \\ icc^* \end{bmatrix} = \sqrt{2}/\sqrt{3} \begin{bmatrix} 1 & 0 \\ -1/2 & \sqrt{3}/2 \\ -1/2 & -\sqrt{3}/2 \end{bmatrix} \begin{bmatrix} ic\alpha \\ ic\beta \end{bmatrix} \quad (2.16)$$

If the reactive power has to be compensated only, it (reactive power) should be sent directly to the reference signal.

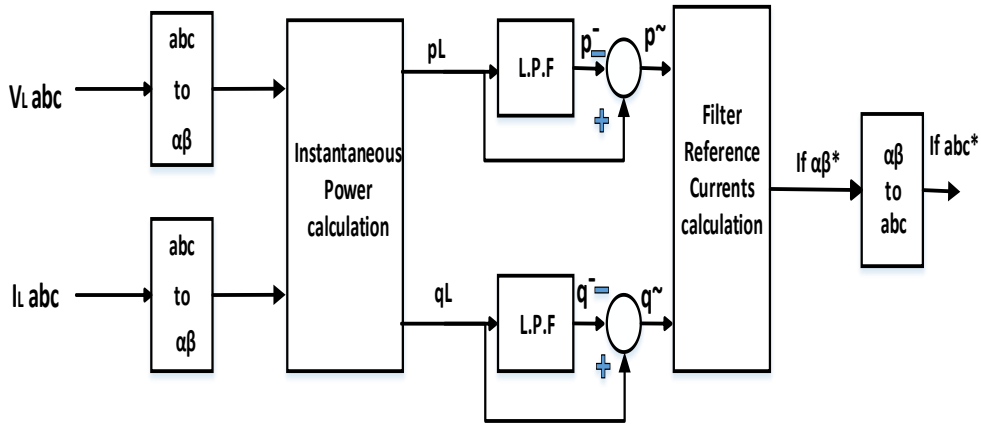


Figure (2.5): Diagram of the p-q theory to eliminate harmonics.

Diagram shown in figure (2.5) is used to eliminate harmonics only. If the power factor has to be improved, the reactive power must consist of two components (\tilde{q}_l & Q_l) so the control diagram become as shown in figure (2.6).

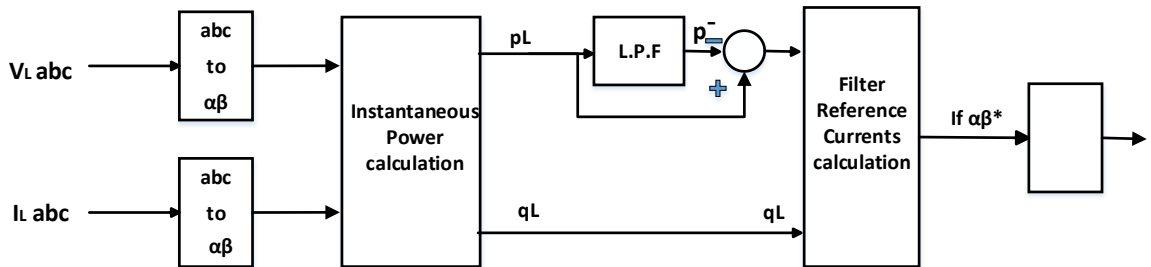


Figure (2.6): Diagram of the p-q theory to eliminate harmonics and improving PF.

2.2.2 Instantaneous Active and Reactive Current Component (id-iq) Method

In this method the instantaneous active and reactive current components of nonlinear load are used to obtain the reference signal. Getting (d - q) current components to separate the harmonic contents from the fundamentals is necessary. The performance in this method is better when there is unbalanced or not ideal voltages [14]. In this method, only the d -axis component should be supplied from the source. The transform is defined by the following equations:

$$\begin{bmatrix} id \\ iq \\ io \end{bmatrix} = \sqrt{\frac{3}{2}} \begin{bmatrix} \cos\theta & \cos(\theta - \frac{2\pi}{3}) & \cos(\theta + \frac{2\pi}{3}) \\ -\sin\theta & -\sin(\theta - \frac{2\pi}{3}) & -\sin(\theta + \frac{2\pi}{3}) \\ 1/\sqrt{2} & 1/\sqrt{2} & 1/\sqrt{2} \end{bmatrix} \begin{bmatrix} ia \\ ib \\ ic \end{bmatrix} \quad (2.17)$$

Where, θ is the angular position of the synchronous reference.

θ is a linear function of the fundamental frequency. This angle is turning in a synchronous constant speed with the three phase voltage. The harmonic current component can be separated from the load currents using low pass filter. The load currents contain two components as following [15]:

$$idl = \widetilde{il}d + \overline{il}d \quad (2.18)$$

$$iq_l = \widetilde{il}q + \overline{il}q \quad (2.19)$$

$\overline{il}d$ and $\overline{il}q$ are average terms and $\widetilde{il}d$ and $\widetilde{il}q$ are oscillatory terms .

The following can be noticed [15]:

- The average current represents the first harmonic (fundamental) current under sinusoidal and balanced condition.
- The oscillating terms are related to all higher harmonics.

The reference signal will be generated by using i_{ql} (two components) to compensate the reactive power and improve the power factor and will also contain the alternative component of id_l (\widetilde{id}) to eliminate harmonics.

The reference signal of the active power filter (APF) becomes:

$$\begin{bmatrix} id^* \\ iq^* \end{bmatrix} = \begin{bmatrix} \widetilde{id} \\ ilq \end{bmatrix} \quad (2.20)$$

The inverse park transform is used to get the reference signal of the APF currents in three phase system as following:

$$\begin{bmatrix} ifa \\ ifb \\ ifc \end{bmatrix} = \frac{\sqrt{3}}{2} \begin{bmatrix} \cos\theta & -\sin\theta \\ \cos(\theta - \frac{2\pi}{3}) & -\sin(\theta - \frac{2\pi}{3}) \\ \cos(\theta + \frac{2\pi}{3}) & \sin(\theta + \frac{2\pi}{3}) \end{bmatrix} \begin{bmatrix} id^* \\ iq^* \end{bmatrix} \quad (2.21)$$

To determine the angular position of the synchronous reference, a phase locked loop (PLL) can be used as shown in figure (2.7)

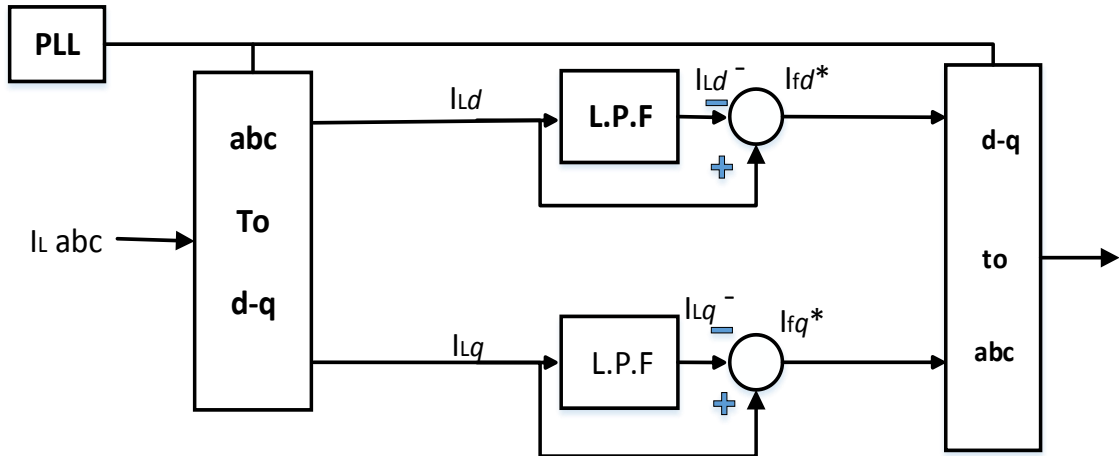


Figure (2.7): Reference current extraction with *id-iq* method.

2.3 Control of the Active Power Filter

It is important to improve the control methods of the SHAPF to get better results such as decreasing the value of THD, improving the P.F of the system, or improving the performance of the SHAPF when the non –linear loads change. There are two control methods to control the APF to compensate the harmonic currents which depend on the measured current:

- Direct Control Method.
- Indirect Control Method.

2.3.1 Direct Control Method.

This method depends on the load currents and the reference signal which will be used to compensate harmonics is extracted from the load currents.

In this case, the SHAPF will generate the currents which don't depend on the source currents but only on the load current which mean that the errors in the measurements or control may appear in grid current as unfiltered harmonics. But in the other hand, large number of sensors is used and system stability will be achieved [16].

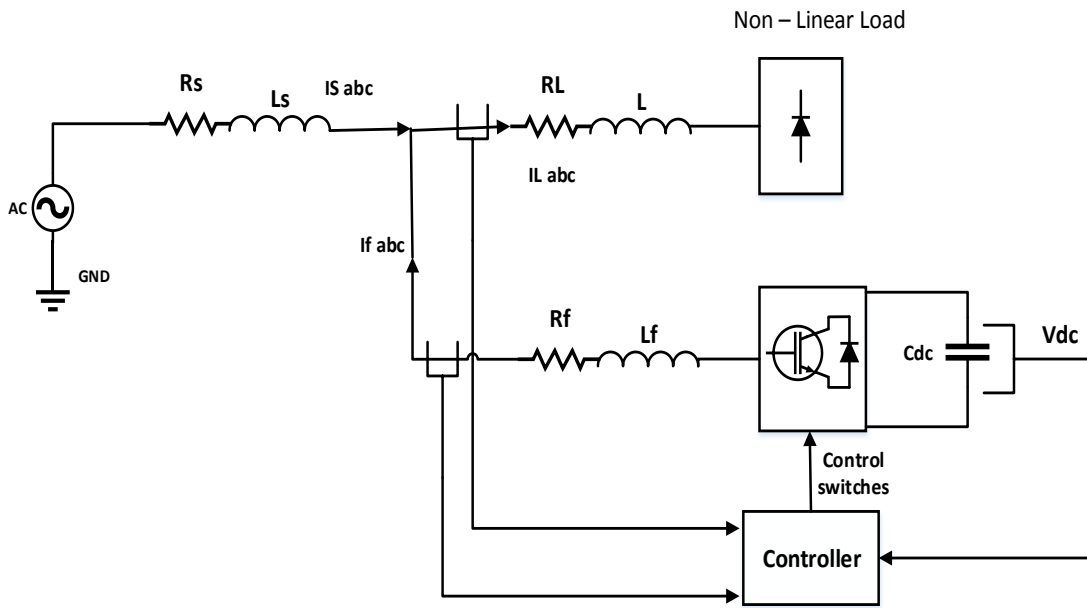


Figure (2.8): Direct control method.

Referring to the figure (2.8), voltages equation can be found as following:

$$\mathbf{V}_f(s) = \mathbf{V}_s(s) + s\mathbf{L}_f \mathbf{I}_f(s) + \mathbf{R}_f \mathbf{I}_f(s) \quad (2.22)$$

The filter current becomes:

$$\mathbf{I}_f(s) = \frac{\mathbf{V}_f(s) - \mathbf{V}_s(s)}{s\mathbf{L}_f + \mathbf{R}_f} \quad (2.23)$$

The control loop of the system becomes as shown in figure (2.9).

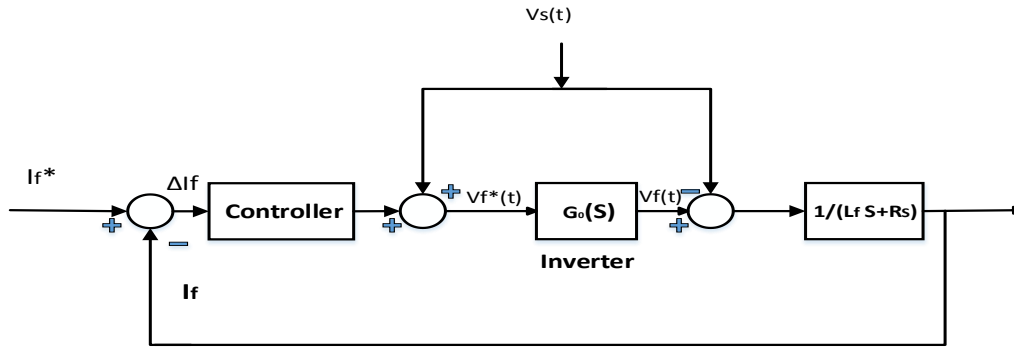


Figure (2.9): Structure of current control loop.

The output voltage of the inverter should equal the reference signal so the transfer function of the inverter should be 1.

Figure (2.10) shows the diagram of the direct control method of parallel active power filter.

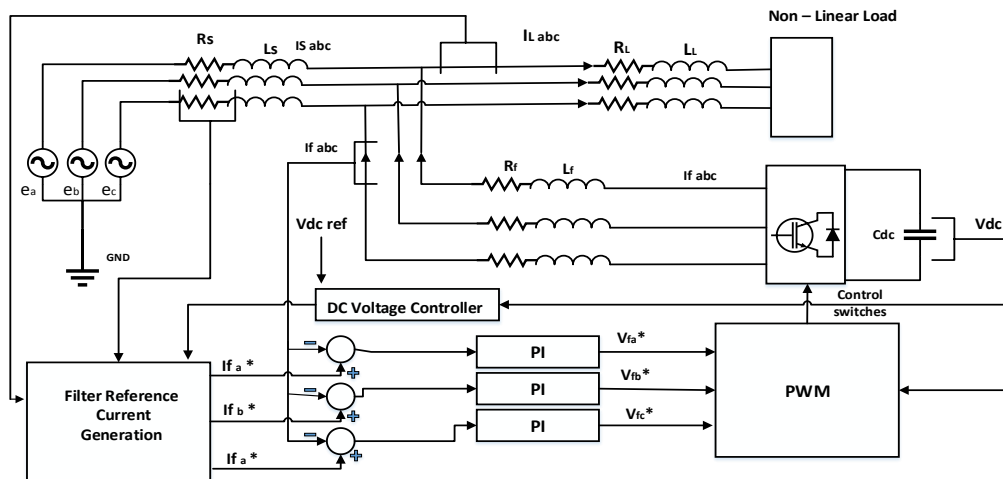


Figure (2.10): Direct control method of SHAPF.

2.3.1.1 Control in the Three Phase Reference.

The PI controller is widely used in current regulation because of its simplicity [17]. Figure (2.11) shows the diagram of the current regulator using PI controller.

A transfer function can be driven from figure (2.11) as following:

$$\mathbf{H_{CL}} = \frac{K_{pi} s + K_{ii}}{L_f s^2 + (R_f + k_{pi})s + K_{ii}} \quad (2.24)$$

Equation (2.24) can be written as following:

$$\mathbf{H_{CL}} = \frac{\left(2\xi\omega_c - \frac{R_f}{L_f}\right)s + \omega_c^2}{2\xi\omega_c s + \omega_c^2 + s^2} \quad (2.25)$$

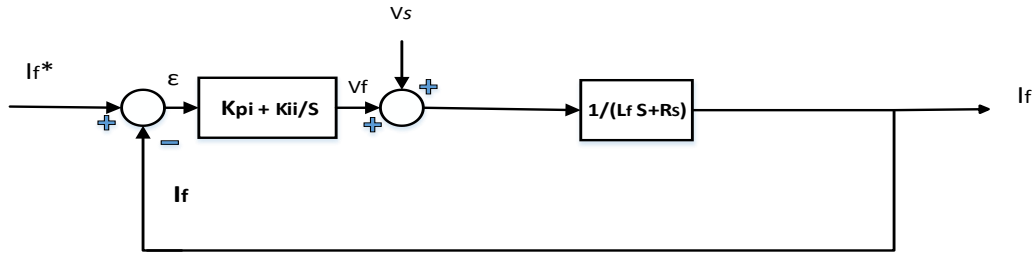


Figure (2.11): PI current controller loop.

To get a suitable dynamic response, the value of damping ratio should equal 0.707.

The constants of controller can be calculated from equations (2.26 – 2.28).

$$K_{pi} = 2\xi\omega_c L_f - R_f \quad (2.26)$$

$$K_{ii} = L_f \omega_c^2 \quad (2.27)$$

$$\omega_c = 2\pi f_c \quad (2.28)$$

2.3.1.2 Control in the Synchronous Frame Reference d-q

In this method, the PI controller is designed to use the synchronous reference d-q instead of using three phase reference. Figure (2.12) shows SHAPF controlled using synchronous frame reference d-q method.

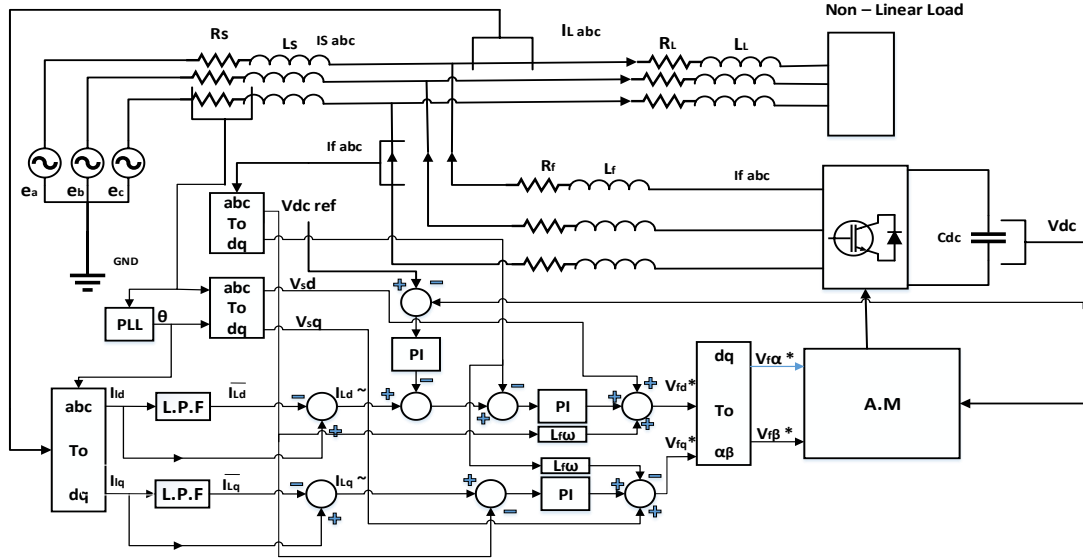


Figure (2.12): Direct control using PI controllers in Synchronous Reference.

2.3.2 Indirect Control of the Active Power Filter

This method interests in source currents without measuring or interesting in the filter currents. Sinusoidal reference current is generated for the grid then this reference will compared to the measured current and the error will fed to current controller to generate pulses to the SHAPF. In this method, the control is less complicated and fewer sensors are needed than direct method. The diagram of indirect method is shown in figure (2.13) [16].

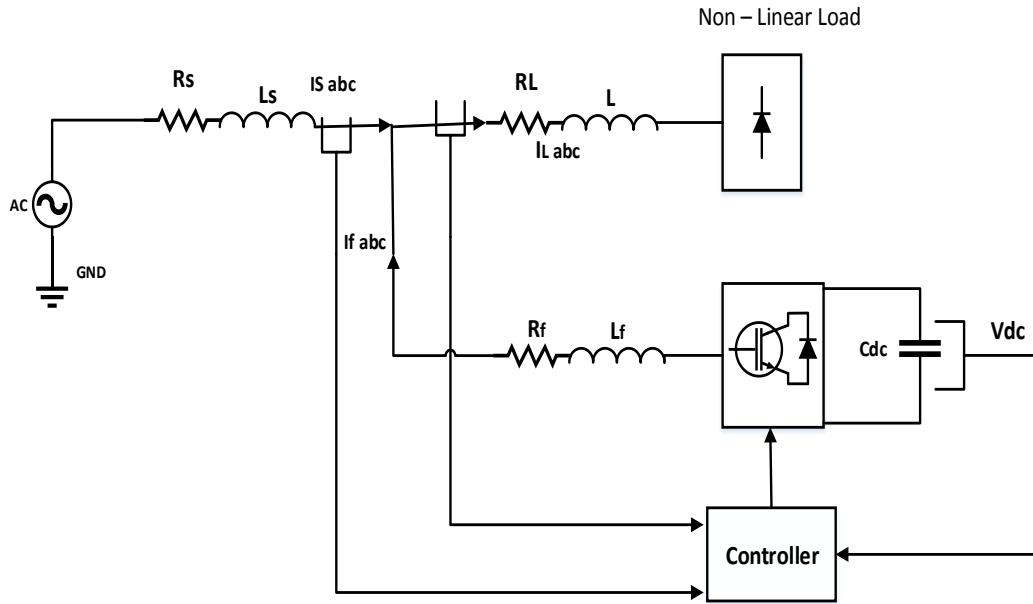


Figure (2.13): Diagram of indirect method control.

2.3.2.1 Grid Current Reference Generation

The grid reference currents are generated in same way used to generate the reference currents of the filter. Many methods used to identify grid currents. Some of these methods depend on PQ theory [12], d-q theory [14], and methods which depend on DC voltage controller.

2.3.2.1.1 PQ Theory Based Algorithm.

This method depends on the instantaneous active power. When using indirect method the direct term (DC term) is reserved to generate grid currents and the alternative component deleted. The reactive power has to be eliminated also so, this method allows compensating the harmonic current and the reactive power at the same time [12].

This method can be explained by the following steps:

Assume the voltages at point PCC v_{sa}, v_{sb}, v_{sc} and the load currents i_{La}, i_{Lb}, i_{Lc} , the following equations can be obtained:

$$\begin{bmatrix} V_{s\alpha} \\ V_{s\beta} \end{bmatrix} = \sqrt{\frac{3}{2}} \begin{bmatrix} 1 & -\frac{1}{2} & -\frac{1}{2} \\ 0 & \frac{\sqrt{3}}{2} & -\frac{\sqrt{3}}{2} \end{bmatrix} \begin{bmatrix} V_{sa} \\ V_{sb} \\ V_{sc} \end{bmatrix} \quad (2.40)$$

And

$$\begin{bmatrix} i_{l\alpha} \\ i_{l\beta} \end{bmatrix} = \sqrt{\frac{3}{2}} \begin{bmatrix} 1 & -\frac{1}{2} & -\frac{1}{2} \\ 0 & \frac{\sqrt{3}}{2} & -\frac{\sqrt{3}}{2} \end{bmatrix} \begin{bmatrix} i_{La} \\ i_{Lb} \\ i_{Lc} \end{bmatrix} \quad (2.41)$$

The instantaneous active power can be written as bellow:

$$P_l = V_{s\alpha} i_{l\alpha} + V_{s\beta} i_{l\beta} \quad (2.42)$$

As mentioned previously, the active power consists of two components, the first one is direct power which is related to the fundamental voltage and current and the second one is alternative which is related to the harmonics.

$$P_l = \overline{pl} + \widetilde{pl} \quad (2.43)$$

If we look from the source side, the reference power becomes as following:

$$P_s^* = \overline{pl} + P_{dc}^* \quad (2.44)$$

The direct active power can be separated by using low pass filter.

The grid reference current becomes as following:

$$i_{s\alpha}^* = \frac{V_{s\alpha}}{V_{s\alpha}^2 + V_{s\beta}^2} P_s^* \quad (2.45)$$

(2.46)

The reference currents become as shown below:

(2.47)

Figure (2.14) shows indirect control method diagram based on the instantaneous power theory.

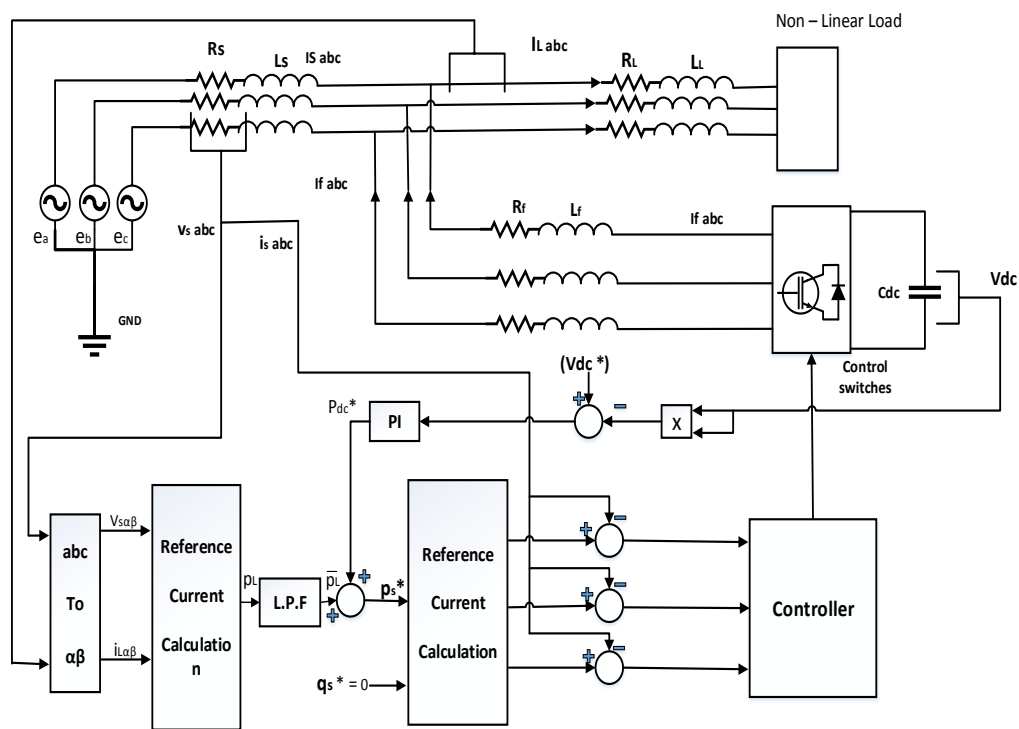


Figure (2.14): Indirect control based on the instantaneous power theory.

2.3.2.1.2 Synchronous Reference Based Method

This method is same as the instantaneous power theory but the difference is that it depends on the calculation of synchronous reference currents. It uses

the load currents and PLL to generate angular position for the voltage, the calculation of direct load current component i_{ld} as following:

$$I_{ld} = \sqrt{\frac{2}{3}} (i_{la} \cos(\omega t) + i_{lb} \cos(\omega t - \frac{2\pi}{3}) + i_{lc} \cos(\omega t + \frac{2\pi}{3})) \quad (2.48)$$

This current consists of two components, direct component and alternating component as shown in the following equation:

$$i_{ld} = i \bar{ld} + i \widetilde{ld} \quad (2.49)$$

The direct current component can be separated by using a suitable low pass filter with a suitable cut-off frequency (nearly 20 Hz) [18], this current relates to the fundamentals of grid.

In this method, i_q can be set to zero which means that this method can compensate the reactive power and the harmonics at the same time. The reference signal can be expressed as following:

$$\begin{bmatrix} isa^* \\ isb^* \\ isc^* \end{bmatrix} = \begin{bmatrix} \cos\theta & -\sin\theta \\ \cos(\theta - \frac{2\pi}{3}) & -\sin(\theta - \frac{2\pi}{3}) \\ \cos(\theta + \frac{2\pi}{3}) & \sin(\theta + \frac{2\pi}{3}) \end{bmatrix} \begin{bmatrix} isd^* \\ isq^* \end{bmatrix} \quad (2.51)$$

Figure (2.15) shows an indirect control method based on the synchronous frame method.

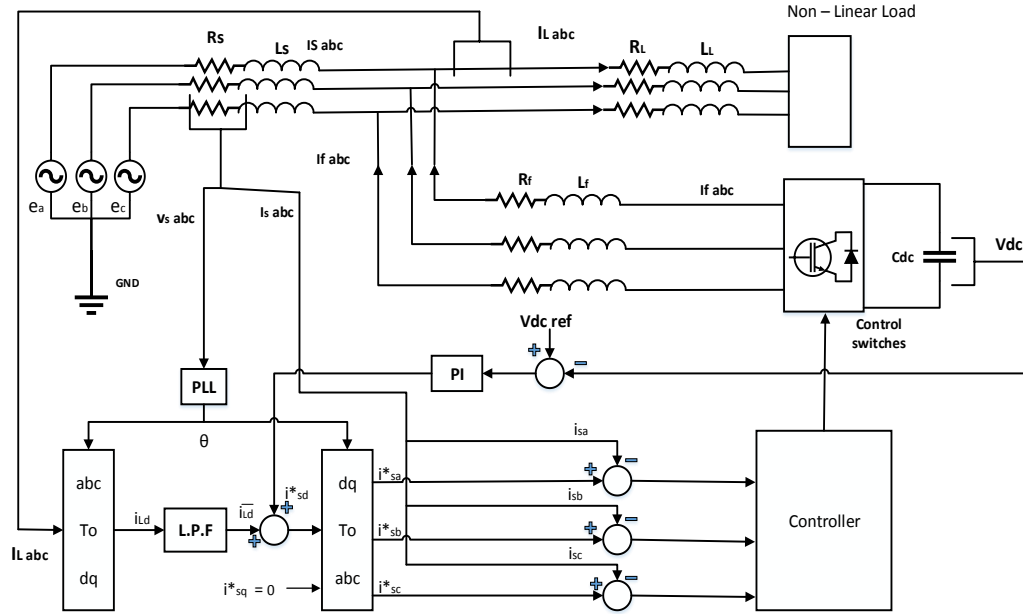


Figure (2.15): Diagram of indirect control based on the synchronous frame method.

2.3.2.2 Design of SHAPF Controller.

The PI controller should be constructed as a part of the active power filter controller to produce the reference signal. The adopted method depends on the direct method control which means that the load current is measured and the harmonics extracted from it. The input of the PI controller is the error between the alternating component of the load current ($\widetilde{i_{Ld}}$ after filtering) and the d- component of the inverter current (I_{invd}). The input of the other PI controller is the error between the currents of the load on the q-axes (I_{Lq}) and the currents of the inverter on the q-axes (I_{invq}) [18].

Let's assume the source voltages (V_a, V_b, V_c) and the inverter output voltages (V_{a1}, V_{b1}, V_{c1}) as shown in Figure (2.16).

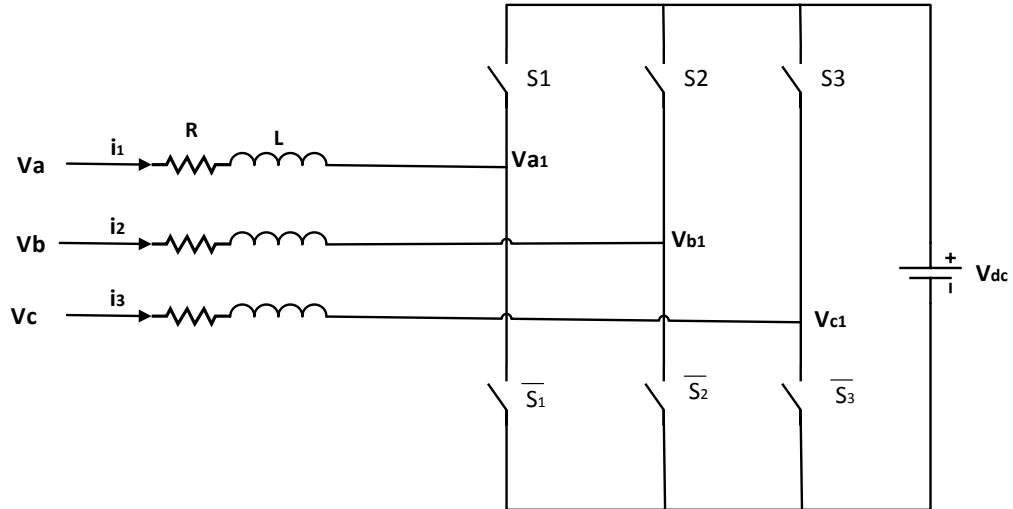


Figure (2.16): Schematic of SAF.

The inverter output is connected to PCC through the resistor R and inductor L. The following voltages of the source equations can be expressed:

$$V_a = i_1 R + L \frac{di_1}{dt} + V_{a1} \quad (2.52)$$

$$V_b = i_2 R + L \frac{di_2}{dt} + V_{b1} \quad (2.53)$$

$$V_c = i_3 R + L \frac{di_3}{dt} + V_{c1} \quad (2.54)$$

Using the transformation to the d-q variables, the above equations become:

$$L \frac{di_d}{dt} = -i_d R + (V_{a_d} - V_{a1d}) - \omega L i_q \quad (2.55)$$

$$L \frac{di_q}{dt} = -i_q R + (V_{a_q} - V_{a1q}) + \omega L i_d \quad (2.56)$$

Or

$$L \frac{di_d}{dt} = -i_d R + V_d$$

$$L \frac{di_d}{dt} = -i_d R + V_q$$

Where,

$$V_d = (V_{a_d} - V_{a_{1d}}) - \omega L i_q$$

$$V_q = (V_{a_q} - V_{a_{1q}}) + \omega L i_d$$

From the previous equations, a model of PI controller can be made as shown in figure (2.17) [18].

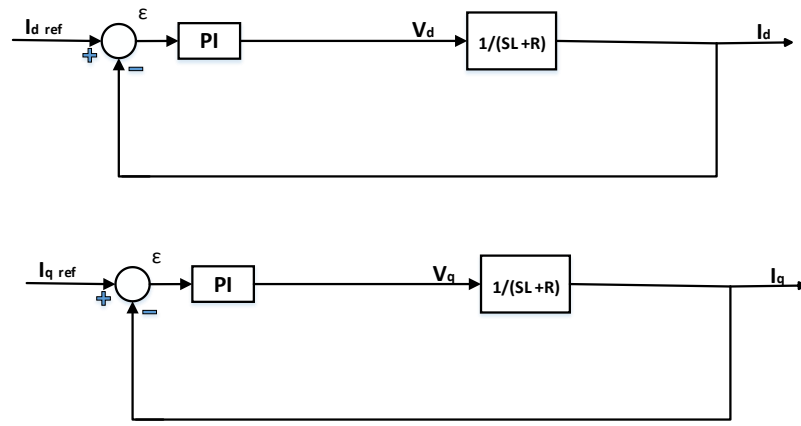


Figure (2.17): Current controller

Let the transfer function of PI controller to be as following:

$$G_{PI}(s) = K_1 + K_2/s \quad (2.61)$$

By comparing the transfer function of the controller with the canonic form of a second order transfer function and assuming the following values:

- Damping factor ξ value equal 0.707 (to insure that the system stable).
- Resistor R equal 3.9Ω .
- Inductor L equal $3.89 * 10^{-3} \text{ H}$.

The values of K_1 & K_2 after solving the equations are as following:

$$K_1 = 450$$

$$K_2 = 30543.9$$

The overall control strategy for SHAPF is shown in figure (2.18) and figure (2.19).

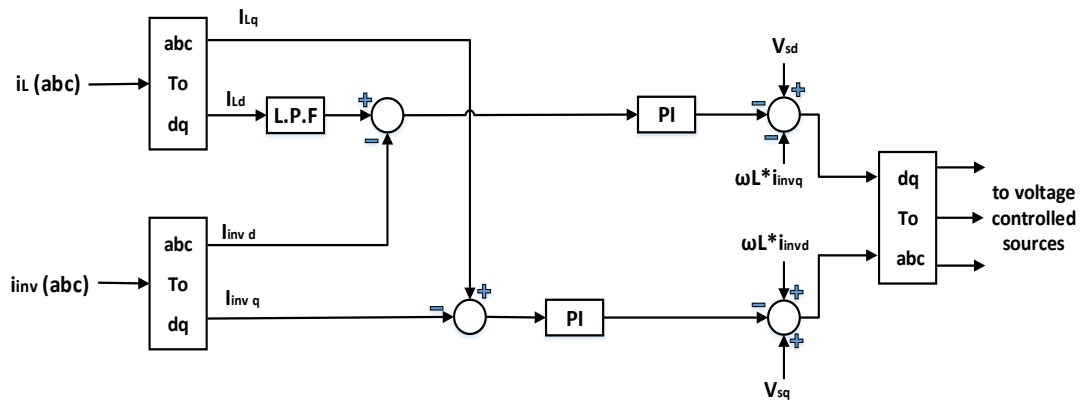


Figure (2.18): Control strategy for the inverter.

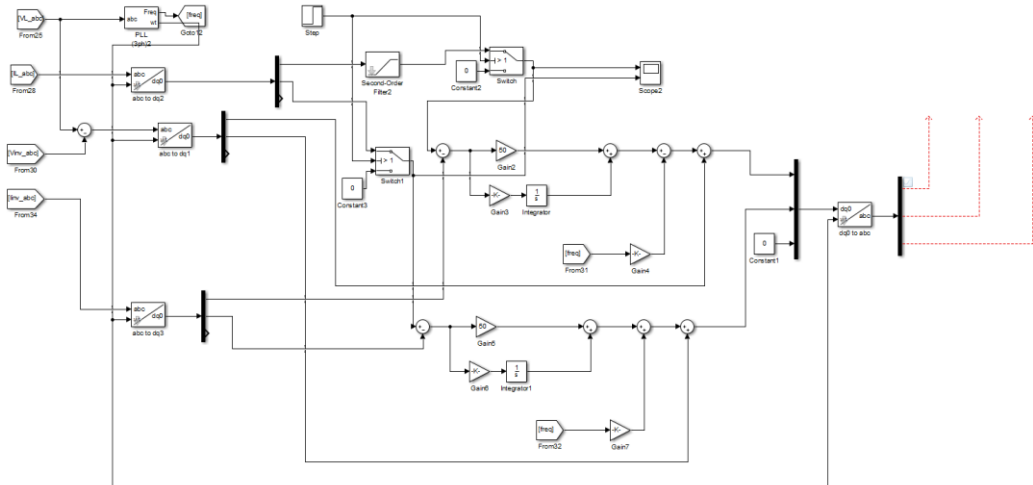


Figure (2.19): Matlab simulink for (SHAPF) controller.

The above control strategy is tested by using MATLAB software.

There are two types of loads; the first is RLC load with parameters shown in table 2.2.

Table 2.2: Load parameters.

Load1	
Active power	3kW
QL	1500
QC	100

The second load is three phase rectifier connected with resistive load and consumes 3kW.

The reference signal produced by the designed controller feeds the controlled voltage sources.

After constructing the system which is shown in figure (2.20) by using MATLAB software, the output source current before and after activating controller is shown in figure (2.21) and figure (2.22). At time 0.5s the inverter starts to work and the output current of the source becomes nearly sinusoidal and the total harmonic distortion (THD_I) decreases from 13.9% to 1.9% which is acceptable (according to IEEE-STD-519-2014) [44].

Figure (2.21): Output source current before and after filtering.

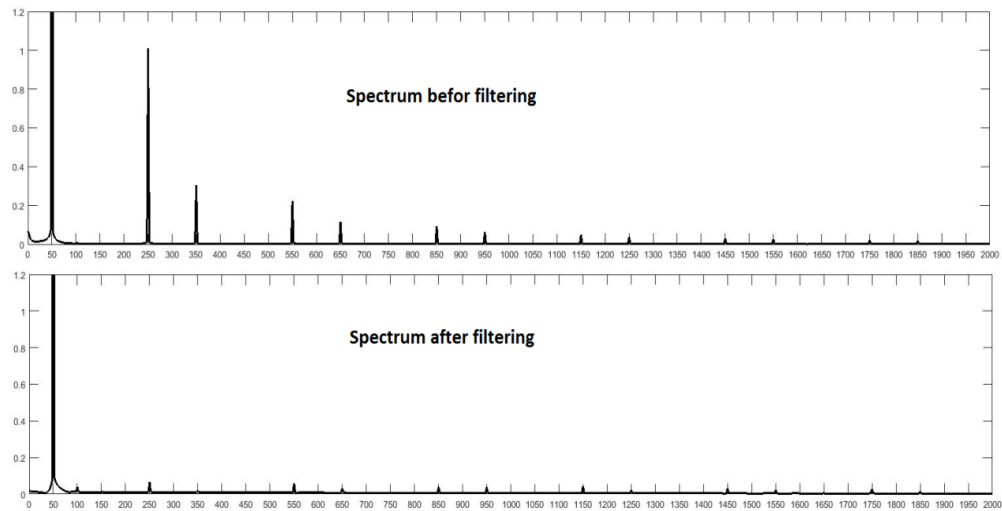


Figure (2.22): Spectrum of source current before and after filtering.

At time 0.5s the filter starts to work and compensates the harmonics so the THD_I becomes 1.9% and at the same time, the filter starts to improve the power factor (P.F) by compensating the reactive power as shown in figure(2.23) and figure (2.24).

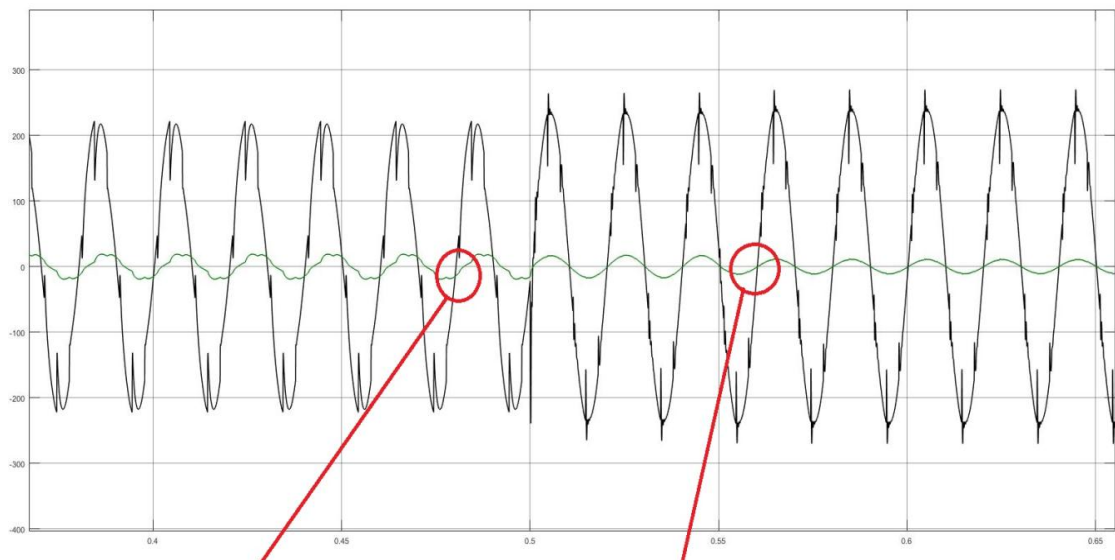


Figure (2.23): Waveform of the voltage and current of the source.

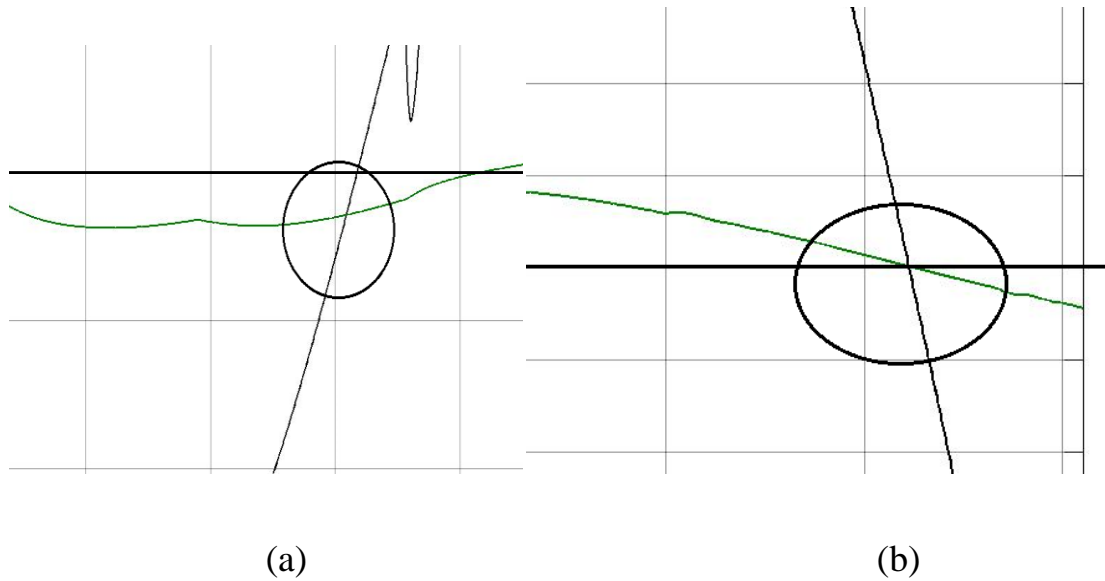


Figure (2.24): Focusing on the crossing point for both cases.

From figure (2.23) and figure (2.24), the crossing point for the current and voltage signals is not on the time axis when the active power filter is off which means that the current lag the voltage or the power factor is less than 1. When the filter starts to work as shown in the figure (2.24/b), the crossing point is at time axis which means that no shifting between current and voltage or the angel is nearly zero so the power factor nearly equal 1.

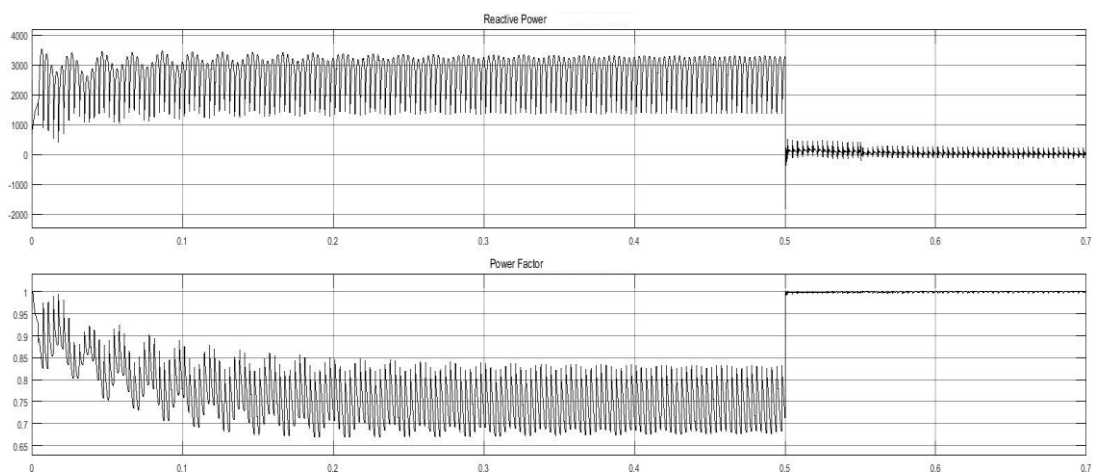


Figure (2.25): Power factor and reactive power produced by source.

Figure (2.25) shows that the source produce all the reactive power needed by the load before the active filter works, but when it starts to work, the new value of the reactive power produced by the source decreases to nearly zero because the active filter compensate the reactive power so the power factor is improved and become nearly 1 after activating the filter.

At time 0.55 s the filter starts to inject real power to the system as shown in figure (2.26).

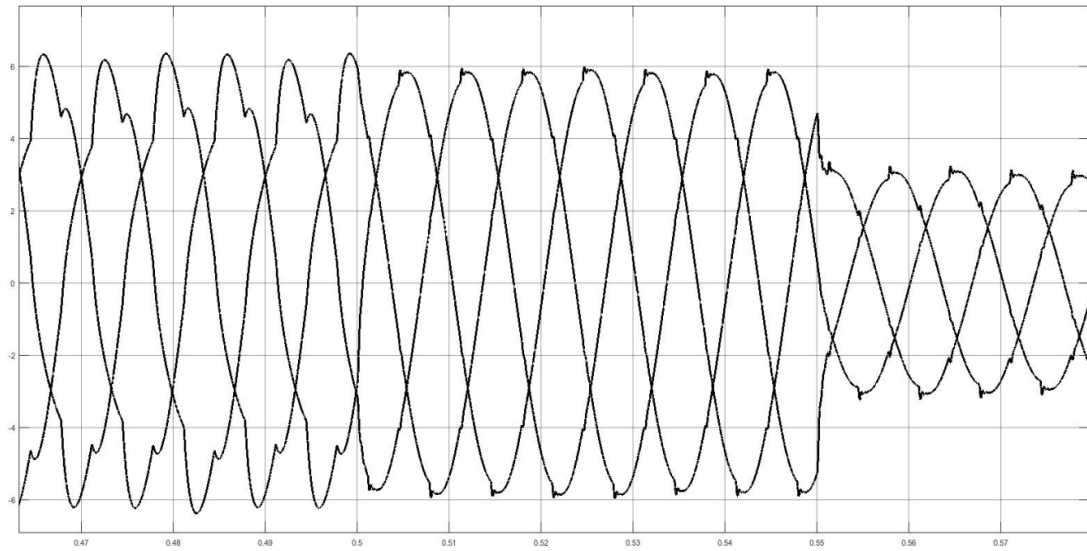


Figure (2.26): Output source current during 3 stages.

Figure (2.26) shows that the source current decreases at time 0.55s because the inverter starts to inject real power at that time.

The designed controller can do three functions as following:

- Mitigating harmonics (reducing the THD from 13.9% to 1.9%).
- Compensating the reactive power and improving the power factor (PF become nearly 1).

- Injecting real power when the produced power by the PV system satisfies the power needed to compensate reactive power and mitigate harmonics.

Chapter Three

Grid Connected PV System with MPPT

3. Grid Connected PV System with MPPT

3.1 Introduction

Solar Energy (SE) is unlimited source of renewable energy that should be harvested and utilized properly as possible. Solar energy can supply the load directly or can be connected with a grid as a distributed generating unit which depends on the situation of the power system or grid. Sometimes it is used to supply far (rural) areas where the ability to connect by the grids is costly and difficult. Improving power quality is another advantage of SE as will be seen in this thesis.

In order to make use of this energy as much as possible, maximum power point tracking (MPPT) method is used to increase the output power produced by SE cells and increase the efficiency of it [19]. The MPPT is very important technique to get maximum power from the Photo Voltaic (PV) panel.

3.2 Photovoltaic Arrangements

3.2.1 PV Cell

Photovoltaic cell is a basic unit which constructs the PV system. It consists of semiconducting material such as germanium and silicon. Silicon is used normally because its advantage over germanium [20]. When the light falls on the surface of semiconductor material, holes and electrons are created

by breaking the covalent bond inside the atom of semiconductor material. So the polarity of terminals becomes positive and negative. The construction of PV cell can either be square or circular.

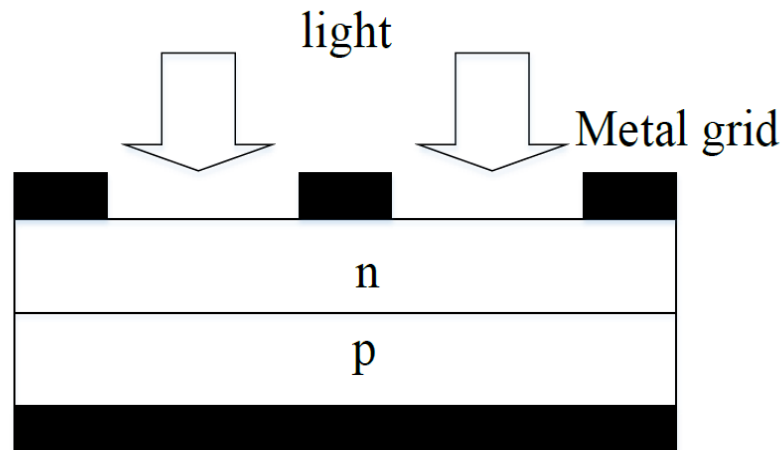


Figure (3.1): PV Cell Structure [20].

3.2.2 PV Module.

A PV cell produce low voltage (around 0.6 V) [20], so many PV cells are connected in series to generate higher voltage and connected in parallel to generate higher current to get needed power for the load. Some problems may appear when connecting PV cells in parallel and series like reversing current when partial or total shading occur [21]. The produced power will be wasted by reverse currents and may cause overheating of the shaded cells. To solve this problem, diodes between cells are used. The efficiency of the module is affected by ambient temperature [22]. At higher temperature the efficiency becomes low so the installers should keep good ventilation for the modules. The efficiency of the cell is always better than

the module due to resistive losses caused by the internal connections of the PV cells in the module.

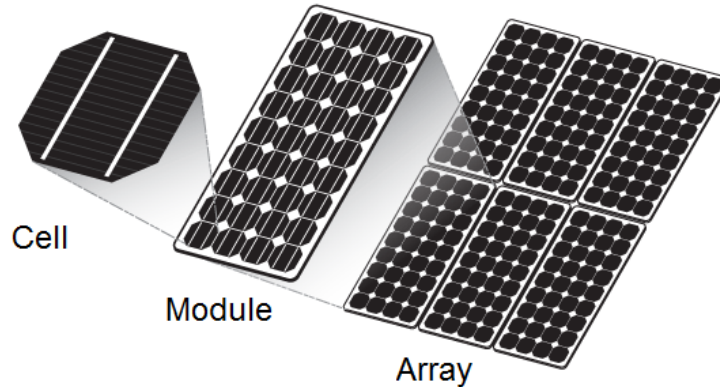


Figure (3.2): Photovoltaic system

3.2.3 Photovoltaic Array.

Photovoltaic array consists of several PV modules connected either in parallel or in series. The connection between modules depends on the needed power for the load. To get higher output voltage, more modules are connected in series and to get higher output current, more modules are connected in parallel. The photovoltaic array uses mostly a power inverter to convert the power from DC to alternating power (AC) that can power many applications.

3.3 Modeling of PV Array

To analyze the model of PV array, it is important to understand the model of PV cell first because it is the basic block which forms the PV array. An equivalent circuit of the cell depends on the physical presentation and

mechanism of a SC which is constructed of a p-n junction that converts solar energy into electrical power.

The equivalent circuit of the PV cell is shown in figure (3.3).

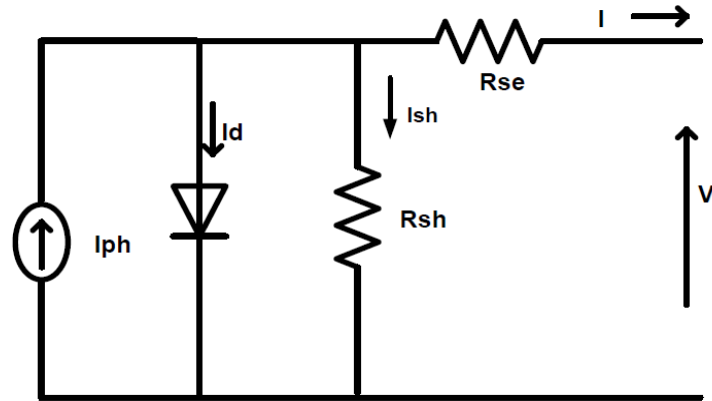


Figure (3.3): Equivalent circuit PV cell [23].

Where,

I_{ph} - Photo current.

I_d - Diode current.

R_{se} - Cell series resistance.

T - Temperature.

V - Cell output voltage.

I - Cell output current.

R_{sh} - Shunt Resistance.

$$I_d = I_{sat} \left(e^{\frac{-q(V+R_{se})}{akt}} - 1 \right) \quad (3.1)$$

Where,

$I_{sat} \approx 50 \text{ nA}$ (for crystalline cell).

a - ideality factor.

Each element of the circuit shown in figure (3.3) has effect on the output power. For example, the series resistance reduces the fill factor and the high value of it may reduce the current in case of short-circuit and the output voltage at MPP decreases. So, by reduction of R_{se} for PV cell application the efficiency will become better [23].

The shunt resistance has also effect on the efficiency. When R_{sh} low, the output power will decrease because the current passing through R_{sh} will increase which means increasing power losses in the PV cell and decreasing the value of the output current and voltage. The output current can be expressed as shown in equations (3.2 to 3.7):

$$I = I_{ph} - I_d - I_{sh} \quad (3.2)$$

$$I = I_{ph} - I_{sat} \left(\exp(q(V + I \times R_{se}) / aKT) - 1 \right) - (V + I \times R_{se}) / R_{sh} \quad (3.3)$$

Where,

q - Electron charge (1.602×10^{-19} coulombs)

a - Ideality factor (its value between 1 and 2).

K - Boltzmann constant ($1.38 \times 10^{-23} \text{ J/K}^0$).

T - Absolute temperature.

The cell temperature and solar radiation affects the I_{ph} as shown in equations (3.4 - 3.7):

$$I_{ph} = \frac{Pin}{hv} \times \alpha \times q \times \eta \times \ell \quad (3.4)$$

Where:

Pin - Incident energy per unit area per second.

hv - Quantum energy of photon.

η - Quantum efficiency.

α - Absorb coefficient.

ℓ - Net displacement of charge.

$$T_c = T_{amb} + \frac{NOCT-20}{800} \times G(t) \quad (3.5)$$

Where,

T_{amb} - Ambient temperature.

NOCT - Normal operation cell temperature.

$$V_{OCT} = V_{OC0} [1 + h_V (T_c - 25^\circ)] \quad (3.6)$$

$$I_{SCT} = I_{SC0} [1 + h_I (T_c - 25^\circ)] \quad (3.7)$$

Where,

h_V - Temperature coefficient for voltage (-3.7×10^{-3}) for crystalline cell.

h_I - Temperature coefficient for current (6.4×10^{-4}) for crystalline cell.

3.4 PV Array Characteristic Curves.

3.4.1 Current Versus Voltage and Power Versus Voltage Curves.

Two values on the current-voltage curve are very important, the first one is the current at maximum power point and the second one is the voltage at maximum power point. The short circuit current I_{sc} is produced when the two terminals of the PV module are shorted, at this point the voltage is zero. The open circuit voltage is produced when the two terminals are open and this voltage is called the open circuit voltage V_{oc} . At this condition the current of the module is zero. When the terminals are connected with load, different values of voltage and current are measured between I_{sc} and V_{oc} . These points form the curve which called current versus voltage curve of PV module as shown in figure (3.4). From current versus voltage curve the power can be calculated and new curve can be obtained which called the Power versus Voltage curve as shown in figure (3.5).

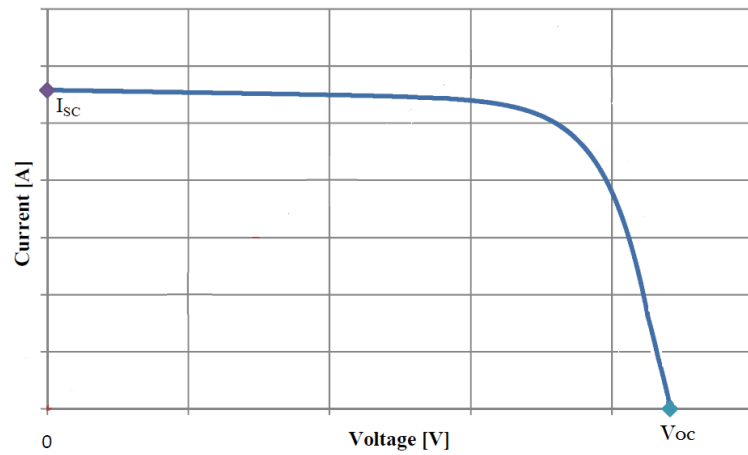


Figure (3.4): Current versus Voltage curve

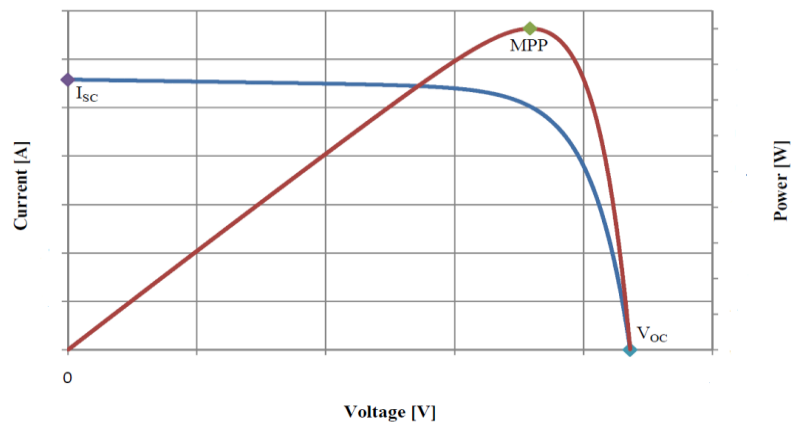


Figure (3.5): Power versus Voltage curve.

3.4.2 Effect of Solar Irradiation on Characteristic Curves.

The solar irradiation affects the I-V curve and P-V curve. When the solar irradiation change then the maximum power point of the solar module will change also [25], so MPPT technique is used to trace the maximum power to increase the efficiency of the module. When more solar irradiation fall on the surface of the solar module, the excitation energy of electrons will increase, so the electrons get higher mobility level which means more

produced power. In this case, the short circuit current will increase as shown in figure (3.6) and the open circuit voltage remains the same [26].

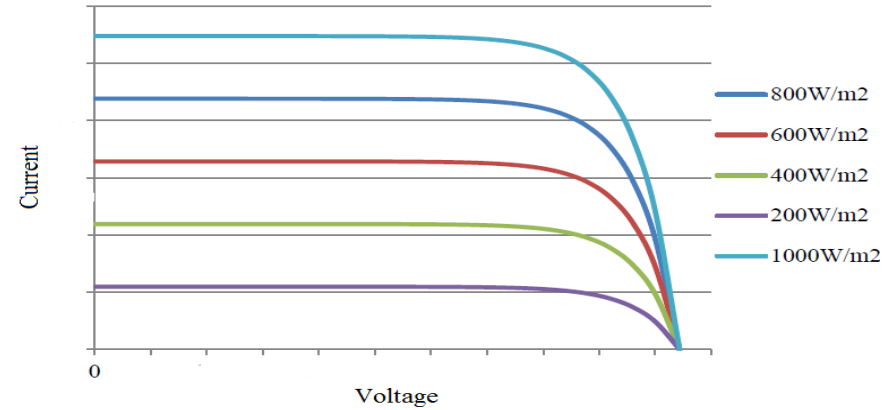


Figure (3.6): Effect of changing solar irradiation on I-V curve.

3.4.3 Effect of Changing Temperature on Characteristic Curves.

The voltage of the PV module is affected by changing the temperature. The open circuit voltage also depends on the temperature as shown in equation(3.6) [27].

From equation (3.6), it can be noticed that when temperature increases, the open circuit voltage decreases because the constant coefficient $h\nu$ is negative but the current increases slightly so the total power decreases. The temperature coefficients are very important parameters of the solar module so the manufacturers should provide it to show how the open circuit voltage is affected by changing the temperature.

Figures (3.7) & (3.8) show the effect of changing temperature on the I-V and P-V curves [28].

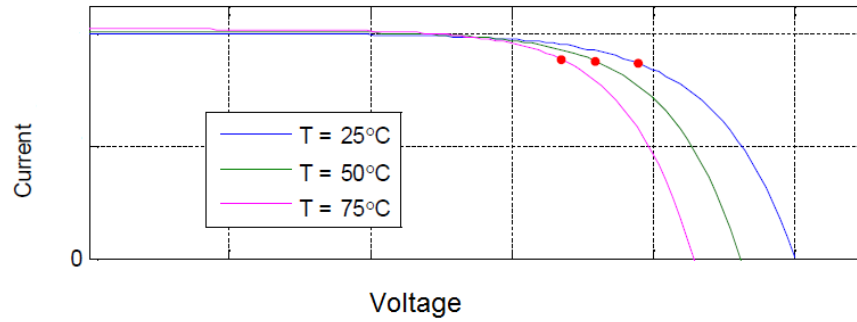


Figure (3.7): I-V curves for many values of temperature.

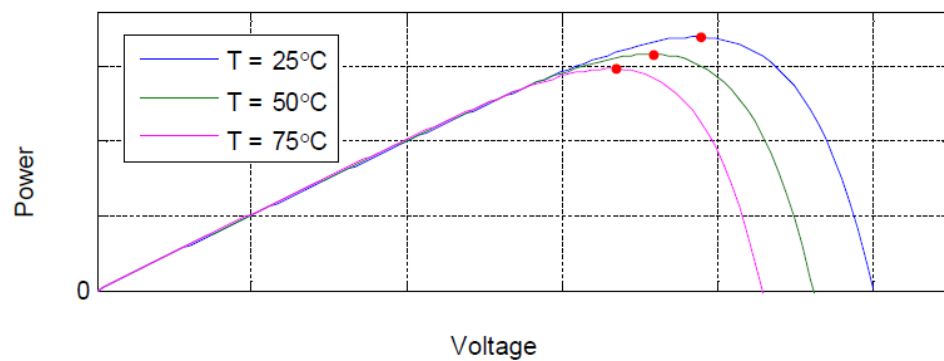


Figure (3.8): P-V curves for different values of temperature.

The atmospheric conditions affect the temperature and the irradiation which are varying during the month or a day; they can vary due to fast changing conditions such as clouds. This means that the solar module needs MPP technique to assure that the module gives maximum possible power always at any condition and to increase the efficiency of the module.

3.5 Maximum Power Point Tracking (MPPT).

Solar irradiation and temperature always change depending upon the days of year, sometimes hours of a day, orientation and latitude of the solar field. So, the amount of solar irradiation which hit the PV array may

change. In this case, the maximum power point tracking technique should be used.

Maximum power point tracking means that the solar cells should give maximum power to improve the efficiency and this happens at certain point on the I-V curve.

The system always should track this point .So; MPPT can be defined as a technique to find the voltage and current to produce maximum power generated by PV panel during different environmental conditions.

To increase the efficiency while using MPPT algorithm, some important features should be taken into account:

- Less price.
- Easy to implement.
- The tracking response is rapid in dynamic condition.
- No oscillations at the MPP during steady state.
- The MPPT algorithm must work with different values of solar irradiation and temperature

3.6 Perturb and Observe (P&O) MPPT Algorithm.

3.6.1 Basic Concept.

P&O technique is the most used type of MPPT algorithms, because its simplicity and minimum parameters required [28]. The basic concept of

this algorithm is that the voltage has to be perturbed regularly and calculating the output power at the same time .After that, the power should be compared with the previous value. If the power increases during the same condition then the increment should be in the same direction. But, if it decreases then the increment should be in the opposite direction. Else, the maximum power achieved when $\frac{\Delta p}{\Delta v} = 0$ [29].

When the algorithm about to reach the maximum point, the oscillation around this point starts. So, the perturbation size should be very small to make the variation of power small. When the atmosphere changes fast, then the lost power may increase because the system can't track the MPP correctly. But, this algorithm stills the most preferred one due to its simplicity [28].

3.6.2 Flow Chart of (P&O) Algorithm.

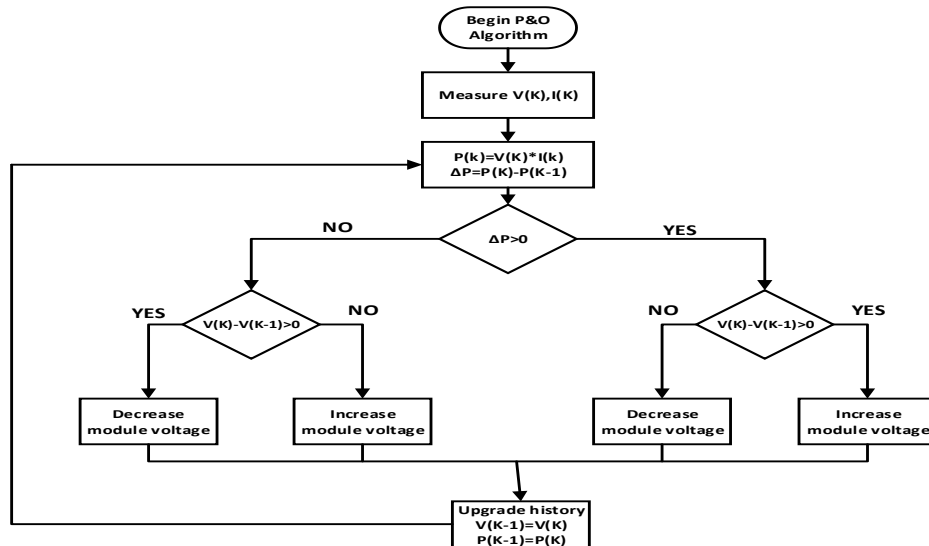


Figure (3.9): Flow chart of (P&O) algorithms [29].

The algorithm works as following steps:

- Tow values of voltage and current are chosen.
- The power is calculated and compared to the previous value.
- If $\Delta p > 0$ and $\Delta v > 0$, this means that the point still in the left side of the curve so the voltage should be increased .
- If $\Delta p > 0$ and $\Delta v < 0$, this means that the point in the right side of the curve so the voltage should be decreased .
- If $\Delta p < 0$ and $\Delta v > 0$,this means that the point in the right side of curve so the voltage should be decreased .
- If $\Delta p < 0$ and $\Delta v < 0$,this mean that the point in the left side of the curve so the voltage should be increased .
- At $\Delta p = 0$,the point is the maximum power point.

3.7 Boost Converter

A boost converter is DC to DC converter which boost-up the input DC voltage to produce desired voltage at output .The boost converter is used also in the PV system to implement the MPPT technique. By using the boost converter, MPPT algorithm can always change the output voltage to check the power if it reaches the maximum value or not. There are three types of converters namely:boost,buck and buck-boost converter. In the PV system, a boost converter is used to step up the PV output voltage .The

boost converter consists of the following elements as shown in figure (3.10).

- Inductor L .
- Controlled switch S .
- Diode D .
- Capacitor C .

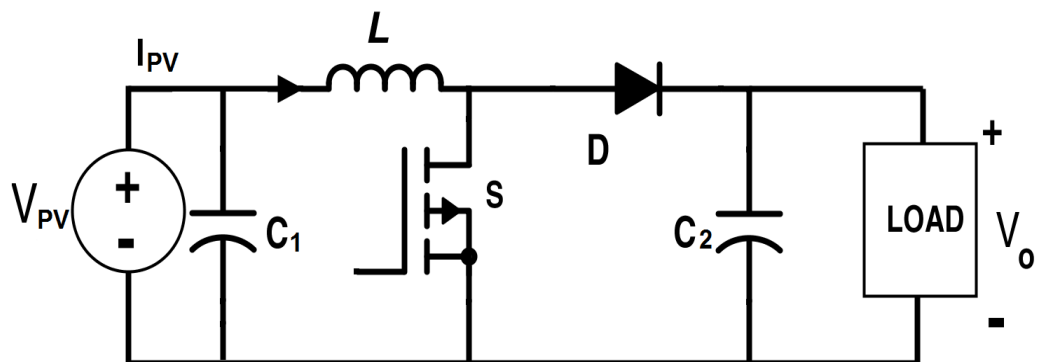


Figure (3.10): Boost converter circuit [45].

Where,

V_{PV} - Input DC voltage (PV).

$C1$ - Capacitor (across the input DC).

D - Diode which is connected in series with load// $C2$.

L - Inductor connected in series with the source.

The output voltage will change depending on the duty cycle. Large values of the capacitor and inductor can be chosen to take voltages and currents as DC values.

3.7.1 The Operation of Boost Converter.

When the switch S is in the on state (as shown in figure 3.9), the current in the inductor L increases linearly and at that time the diode D is off so, this mode is called charging mode .After that the switch S is turned off and the stored energy in L start to flow to the output RC circuit and this mode is called discharging mode.

The relation between input and output voltages is shown in the following equation:

$$V_{in} = (1-D) V_{out} \quad (3.8)$$

It is seen from equation (3.5) that the conversion ratio depends on the duty cycle assuming constant-frequency operation. To control the output voltage to give maximum power, a controller should be added to the boost converter to choose suitable duty cycle to achieve that.

3.7.1.1 Charging Mode of Operation

In this mode, the switch is closed as shown in figure (3.11) , so the inductor start to store the energy as a result the inductor current rises exponentially but it is assumed as a linear current .The load current remains constant

because the capacitor connected parallel with the load will discharge through it during this mode.

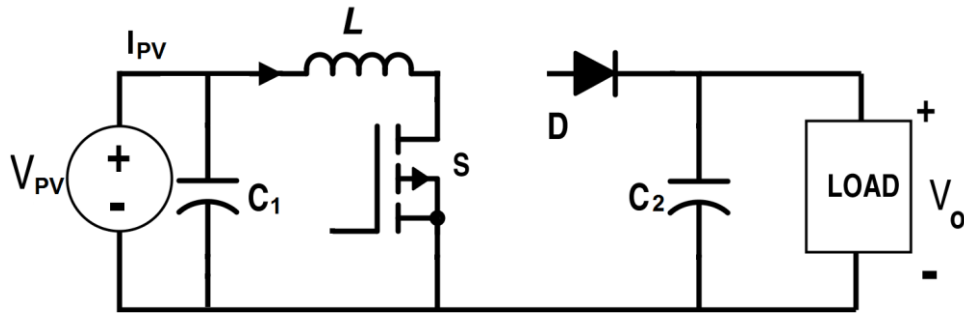


Figure (3.11): Charging mode of boost converter [45].

3.7.1.2 Mode-2 or Discharging Mode of Operation

In this mode the switch is opened and the diode acts as a short circuit as shown in figure (3.12). So the energy which is stored in the inductor will discharge through the load with opposite polarity and at this time the capacitor start to charge again.

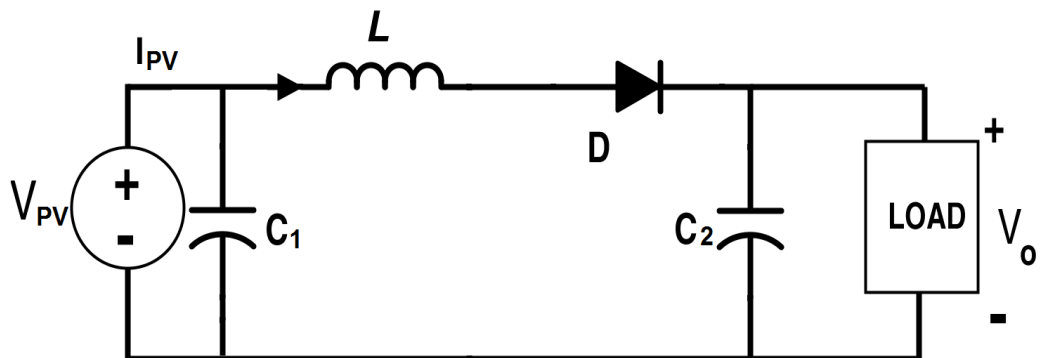


Figure (3.12): Discharging mode of operation [45].

3.7.2 Waveforms.

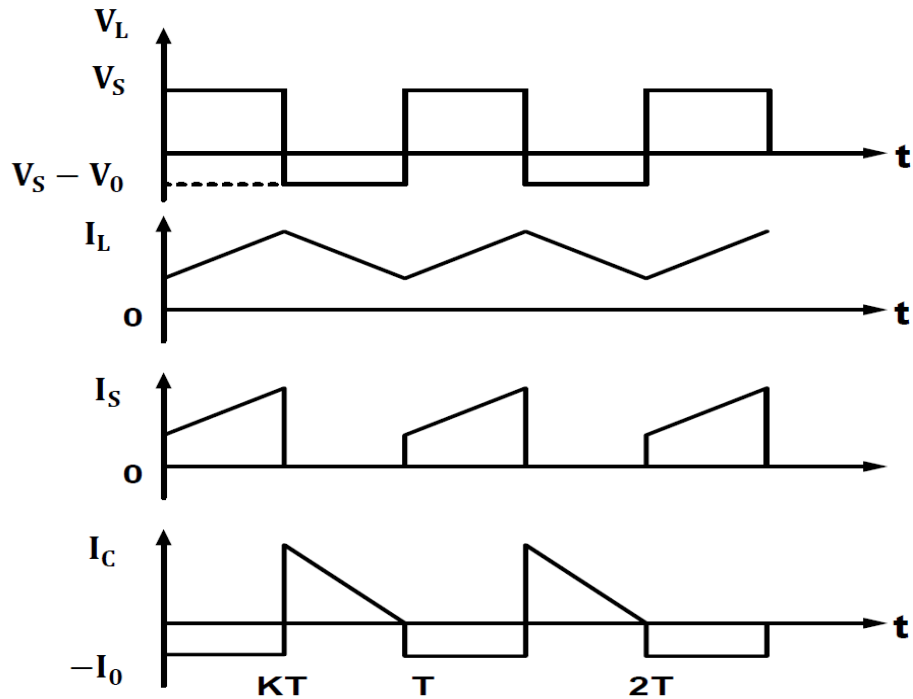


Figure (3.13): Waveforms of boost converter modes [45].

3.8 Design of the System (PV and Boost Converter).

3.8.1 Design of the PV System.

To design the PV system, Mitsubishi electric PV-EE125MF5F module is chosen to build the system with the following specifications shown in the following table:

Table (3.1): Specification of Mitsubishi electric PV-EE125MF5F module at standard conditions.

Mitsubishi electric PV-EE125MF5F model specification	
Maximum Power	125.079
Maximum Power Voltage	17.3
Maximum Power Current	7.23
Open Circuit Voltage	21.8
Short Circuit Current	7.9
Area	$0.9291m^2$

A PV system have to be designed to feed the load with assumed needed energy equal 7kWh per a day and output voltage 75 V which will be stepped up through the boost converter to 108 volt to be connected to the inverter.

The peak power of the PV system should be calculated from the following equation [30]:

$$P_{pv} = \frac{E_L}{\eta_v \eta_R PSH} S_f \quad (3.9)$$

Where,

E_L : energy consumption per day.

PSH : peak sun hours (5.4 in Palestine).

η_v : efficiency of charge regulator (0.92).

η_R : efficiency of inverter (0.9).

S_f : safety] factor (1.15).

Substituting these values in equation (3.6) to calculate the peak PV power as following:

$$P_{pv} = \frac{7}{.9*.92*5.4} * 1.15 = 1.8 \text{ kWp.}$$

To calculate the number of modules needed, the following equation should be used:

$$\text{No. pv} = \frac{P_{pv}}{P_{mpp}} \quad (3.7)$$

$$\text{No. pv} = \frac{1800}{125} = 14.4 \approx 15 \text{ module needed.}$$

To obtain the needed output voltage of the PV system, number of modules which connected in series should be determined. To do this, the following equation should be used.

$$N_s = \frac{\text{needed voltage}}{V_{mpp \text{ for module}}} \quad (3.8)$$

Where N_s : number of modules connected in series.

$$N_s = \frac{75}{17.3} = 4.34 \approx 5 \text{ modules connected in series.}$$

Each string has 5 modules with a voltage of about 86.5 volts.

To determine number of strings connected in parallel, a power of each string should be calculated as following:

$$\text{Power produced by one string} = \text{number of modules} * \text{MPP} \quad (3.9)$$

$$\text{Power produced by one string} = 5 * 17.3 * 7.23 = 625.4 \text{ W.}$$

$$\text{Number of strings} = \frac{\text{total power}}{\text{string power}} \quad (3.8)$$

Number of strings = $\frac{1800}{625.4} = 3.2 \approx 4$ strings connected in parallel.

According to this construction, the peak power of the PV generator will be 2500 W which means that the safety factor is increased to be 1.6.

The needed PV system consist of four strings connected in parallel where each string consists of five modules connected in series as shown in figure(3.14):

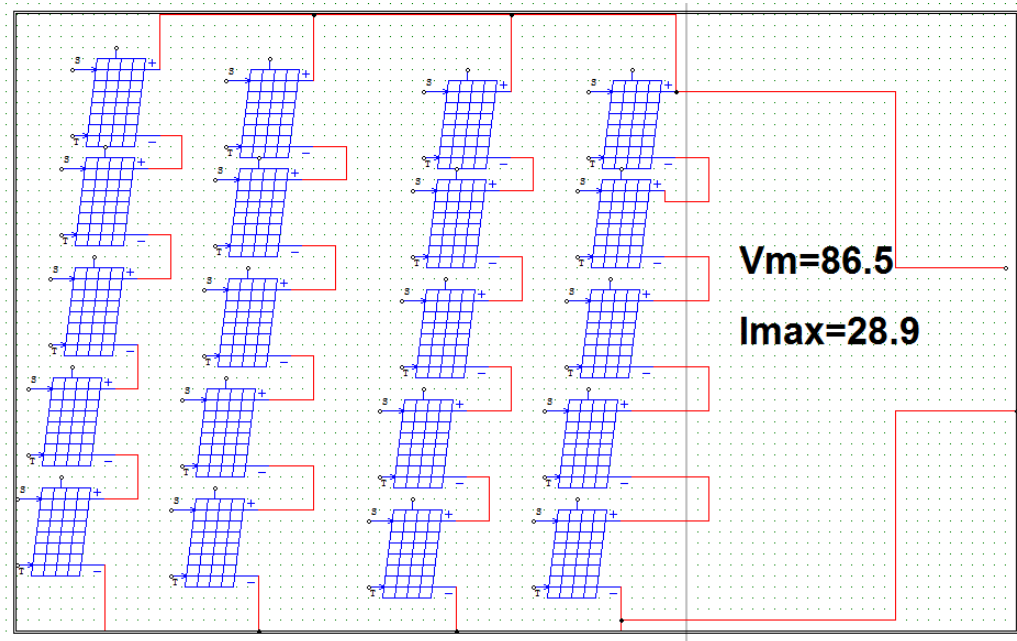


Figure (3.14): The configuration of PV generator.

3.8.2 Calculation of Boost Converter Parameters.

Figure (3.10) shows the circuit of the boost converter. The input is connected with the output of the PV system. The inductance and the capacitor should be calculated. The switching command of the IGBT (S)

assumed to be 10 kHz. The design specifications of boost controller are shown in table (3.2).

The boost converter should receive DC voltage from PV system which varies between 0 to 86 volts and the output voltage of the boost controller is fixed to 108V (DC).

Table 3.2: Specification of boost converter.

Parameter values	
Input Voltage	0-86 V
Output Voltage	108 V
Switching frequency	10 kHz

Depending on the specification for input and output voltages shown in table(3.2), the required duty cycle can be determined by using Equation (3.5).

The value of duty cycle of the boost converter is determined due to the value of the output voltage of the PV system.

The minimum value of Inductor L_{min} and minimum value of capacitor of boost controller have to be determined.

The minimum value of duty cycle obtained when the input voltage of boost converter is maximum.

Equation (3.5) can be rewritten as following:

$$D = \frac{V_0 - V_{in}}{V_0}.$$

$$D_{\min} = \frac{108-86}{108} = 20\%.$$

$$D_{\max} = \frac{108-0}{108} = 1.$$

The minimum value of the inductor can be calculated depending on the following equation :

$$L_{\min} = \frac{D(1-D)^2 R}{2f} \quad (3.9)$$

$$L_{\min} = \frac{0.20(1-0.20)^2 10}{2*10*10^3} = 64 * 10^{-3} \text{ mH}.$$

Let the peak to peak value ripple voltage equal 0.05. The capacitor value can be calculated by using the following equation :

$$C_{\min} = \frac{(V_0)D}{\Delta V R f} \quad (3.10)$$

$$\Delta V = 0.05$$

$$C_{\min} = \frac{108*0.20}{0.05*10*10*10^3} = 4.3 \text{ mF}$$

After completing the design of PV, boost converter and controller, a system is build using MATLAB software, the output voltage of the PV system is shown in the following figure:

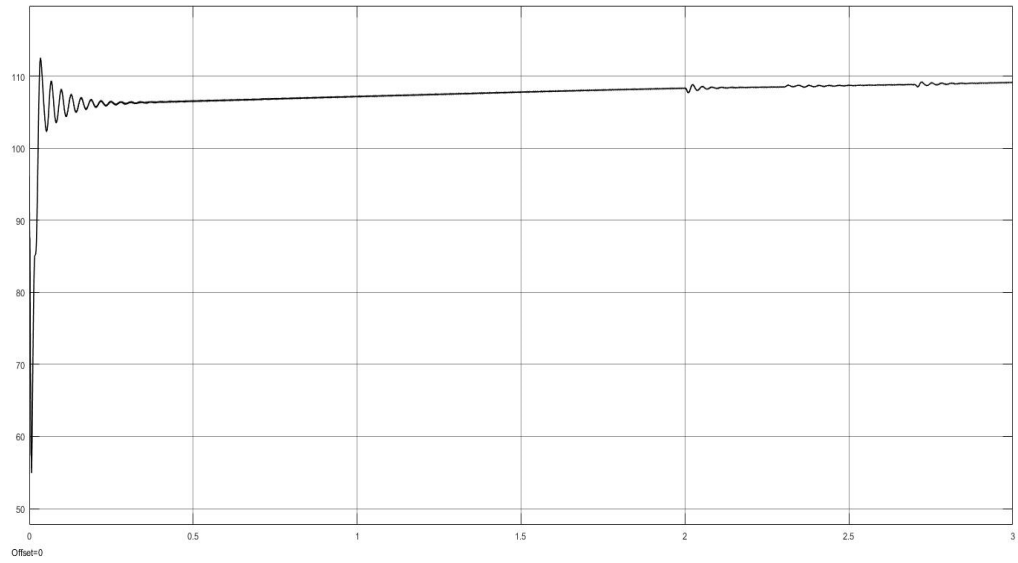


Figure (3.15): Output voltage of the PV system.

Chapter Four

Multilevel Inverter

4. Multilevel Inverter

4.1 Introduction

Inverter is an electrical device that has the ability to convert DC power to AC at needed value of frequency and voltage. The first type of inverters used is the two level inverter. This type suffers from many problems like high switching frequency and losses, many limitations for high power applications, large THD, and high stress on the power switches. For these drawbacks, this type is not suitable when using medium or high power applications or grid. When using a medium or high voltage grid, it is not suitable to connect only one power semiconductor switch directly because it has limited power rating. So, a multilevel power inverter can be used instead of conventional inverter in medium power and voltage situations. A multilevel inverter is not only suitable for interfacing high power applications, but also produces a better output signal with minimum harmonics and nearly the same as reference signal. A multilevel inverter usually used to connect the renewable energy sources such as wind, photovoltaic, and other sources to the grid [31].

The multilevel term means that the levels of the inverter are three or above. Many, topologies are used to design the multilevel inverter. However, to get high power inverter, the construction should use larger number of power switches and DC sources.

The main disadvantage of the multilevel inverters is the great number of power semiconductor switches used. Each switch needs a particular drive circuit. This means more complex and expensive system [31].

4.2 Multilevel Inverter Structures.

The multilevel inverter consists of three levels or more. Sometimes, it is called converter and not inverter because it uses bi-directional switches or can work in both modes as a rectifier or an inverter. When the number of levels increase, the THD will decrease and the performance of the system become better [31].

In a multilevel Voltage Source Inverter (VSI), the voltage of dc-link (V_{DC}) is obtained from any DC source which can produce stable DC power. Series connected capacitors are used as an energy tank to produce many choices of DC voltage values for the inverter as shown in figure (4.1). Each capacitor has voltage V_c as showing in the following equation [31].

$$V_c = V_{DC} / (n-1) \quad (4.1)$$

Where:

n - Number of level.

A schematic diagram of different types of inverters (one phase leg) can be shown in figure (4.1) with different number of levels, the semiconductor switches can move to different positions to get certain DC value .The

output voltage of two-level inverter have two values while the n-level inverter will produce an output voltage with n voltage values.

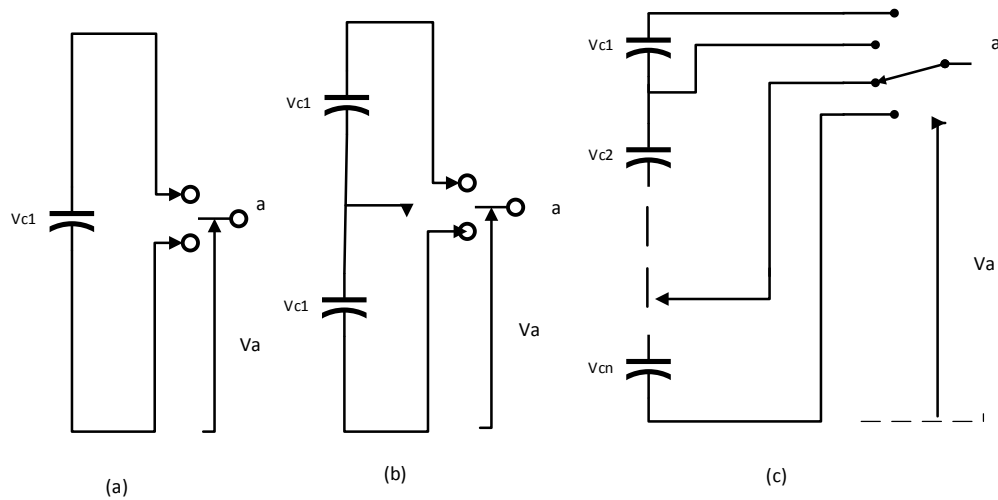


Figure (4.1): One phase leg inverter with (a) two levels, (b) three levels, and (c) n levels [31].

4.2.1 Diode-Clamped Multilevel Inverter.

The diode clamped multilevel inverter topology is commonly used. The diode is used to clamp the DC voltage to get many values or steps in the output voltage [32].

For example, a three-level inverter which uses diode clamped topology consists of two couples of diodes and switches. Each pair of switches work complementary and the diodes used to get mid-point voltage. In this topology, the DC bus is used by each of three phases of the inverter and divided into three levels by using two capacitors. The voltage stress across each switching device is limited to V_{dc} through the clamping diodes D1

and D2 as shown in figure (4.2). The output voltage across each capacitor is $V_{DC}/2$ where ($V_{C1}=V_{C2}=V_{DC}/2$) [31].

When using three level inverter (as shown in figure 4.2), there are three states of the switches to get three different possible values of the output. At any time, a set of two switches should be on.

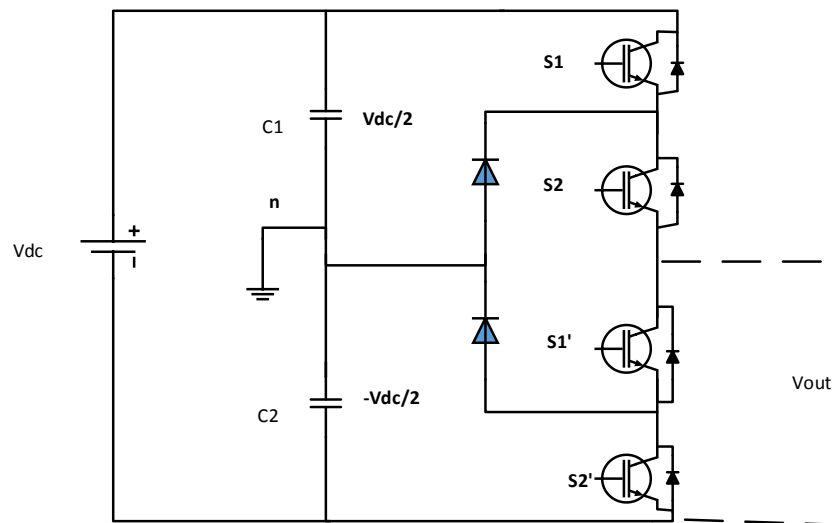


Figure (4.2): Three level inverter using diode-clamped inverter topology [31].

Table (4.1) shows switching states of the three level diode-clamped inverter.

Table 4.1: States of the three level diode-clamped inverter.

Switch status	State	Voltage
S1=ON,S2=ON S1'=OFF,S2'=OFF	S=+ve	$V_o=V_{dc}/2$
S1=OFF,S2=ON S1'=ON,S2'=OFF	S=0	$V_o=0$
S1=OFF,S2=OFF S1'=ON,S2'=ON	S=-ve	$V_o=-V_{dc}/2$

In general, to design an N level diode clamped inverter, $2(N-1)$ switching devices are needed for each leg, $(N-1)$ DC link capacitors and $(N-1) \times (N-2)$ clamping diodes are required [32]. The quality of the output voltage depends on the number of levels. Increasing the levels means high quality waveform and closer to sinusoidal or reference signal. However when the number N become higher, the number of switching devices and clamping diodes will increase and make the designed inverter more complex.

4.2.1.1 Advantages and Disadvantages of DCMLI.

The advantages of DCMLI are listed below:

1. A common DC bus is shared for all of the phases.
2. The capacitors can be pre-charged as a group.
3. Low harmonics when using high number of levels.

The Disadvantages of DCMLI are listed below:

1. If the monitoring and control are not accurate, the DC level may decrease or discharge [32].
2. To get high quality output, the number of clamping diodes needed is high which makes the system complex.

4.2.2 Flying Capacitor Multilevel Inverter.

The idea of the capacitor clamped inverter which known also as flying capacitor was proposed by Foch and Meynard in 1992 [33]. The structure of

this type of inverters is same as in the diode-clamped type but instead of using clamping diodes, capacitors are used in their places. The flying capacitors are connected in series connection, where the voltage on each capacitor differs from that of the next capacitor. The voltage steps in the output waveform depending on the two adjacent capacitor legs chosen. Figure (4.3) shows the three-level capacitor clamped inverter structure.

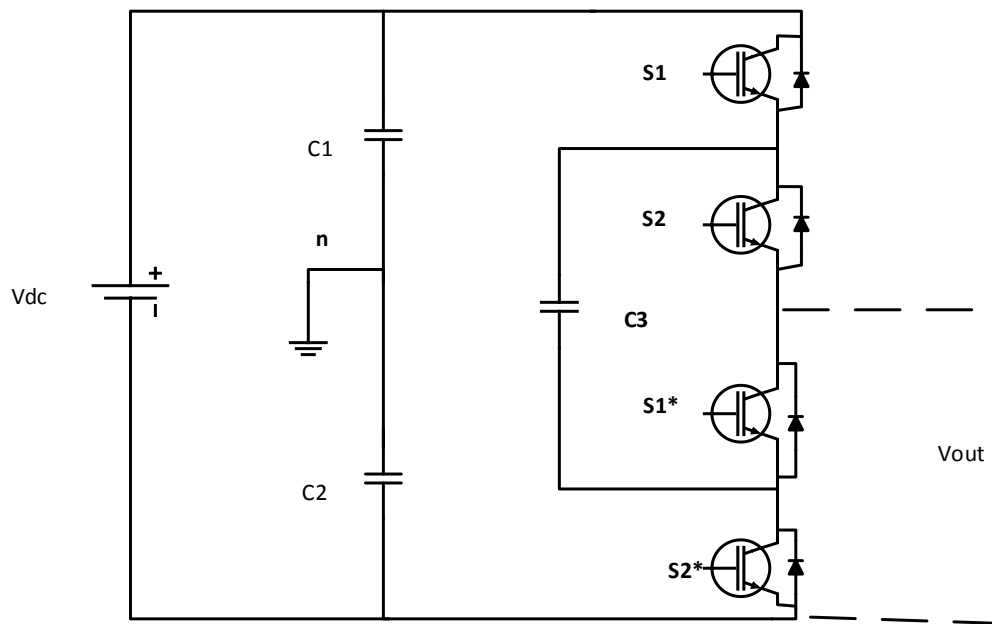


Figure (4.3): Circuit topology for capacitor-clamped multilevel inverter (three levels) [31].

4.2.2.1 Advantages and Disadvantages of (FCMLI).

The advantages of FCMLI are listed below:

- 1- In the capacitor-clamped voltage topology, the capacitors which shared the same leg are charged to different voltage values which mean more levels can be used. But in diode clamped topology, the series string of capacitors have the same voltage.

- 2- The inverter has the ability to ride through deep voltage sags and short duration outages.

The disadvantages of DCMLI are listed below:

- 1- The capacitors have to be charged initially before any modulation which complicates the control and modulation process.
- 2- The control becomes very complicated when using large number of capacitors.
- 3- The startup and precharging the capacitors is complex.
- 4- Using capacitors make the converter more expensive than using diodes.

4.2.3 Cascaded Multilevel Inverter.

Another type of multilevel inverters is the Cascaded Multilevel Inverter (CMI) which called also series H-bridge inverter. The H-bridge inverter was proposed in 1975 [6].The CMI has been utilized in a wide range of applications especially high-power applications because its modularity and flexibility [35]. Each phase of the inverter consists of a series of single-phase full bridges. To build three-phase output AC waveform, CMI should have three phase legs of series H-bridge converters. The voltage level when using this topology is easily scaled because this topology depends on series power conversion cells. Each full bridge converter is provided by DC supply separately which achieved by using PV system, diode rectifiers or other dc sources.

4.2.3.1 Operation of CMLI.

The topology of this type of converters is based on the series connection of H-bridge converters with separate DC sources as shown in figure (4.4).

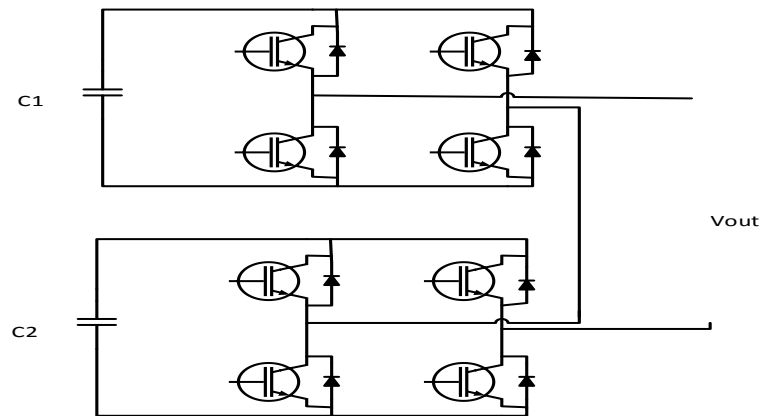


Figure (4.4): Three-level Cascaded Multilevel Inverter [31].

The output phase voltage is made of the voltages generated by the different cells. In a 3-level inverter each single-phase full-bridge converter produces three voltage levels at the output: $+V_{DC}$, 0, $-V_{DC}$ (positive DC voltage, zero, and negative DC voltage). This can be achieved by controlling the power switches to produce the desired output. The produced output AC voltage varies from $+V_{DC}$ to $-V_{DC}$ with three levels.

The output voltage of the three-phase system for the cascaded converter can be connected in either delta (Δ) or wye (Y) configurations.

4.2.3.2 Advantages of CMLI.

The advantages of DMLI are listed below:

- 1- Modularity can be achieved for control. Unlike capacitor clamped and the diode clamped inverter where the modulation for individual phase legs must be achieved by a central controller, the H-bridge cells of a cascaded structure can be modulated separately.
- 2- The components used to build this type are less than other inverters to produce the same output voltage levels.
- 3- Soft-switching control can be used in this topology.

4.3 Multilevel Inverter Design.

H-bridge with 27 level inverter is chosen for this project for the following reasons:

- 1- Increasing the number of levels (27) will decrease the distortion in the output waveform.
- 2- It is more suitable to high-power, high-voltage applications than the conventional inverters.
- 3- Easy to control than other types of inverters because it consists of cells which can be modulated separately.
- 4- By increasing the number of levels, the voltage stress on the switches will decrease.
- 5- Switches can be controlled by using Soft-switching.

The inverter consists of three H-bridges with three unequal distributed DC sources with relation (1:3:9) as shown in figure (4.5)

The DC sources have the following values:

Table 2: The DC sources of the Inverter.

Source 1	Source 2	Source 3
36	108	324

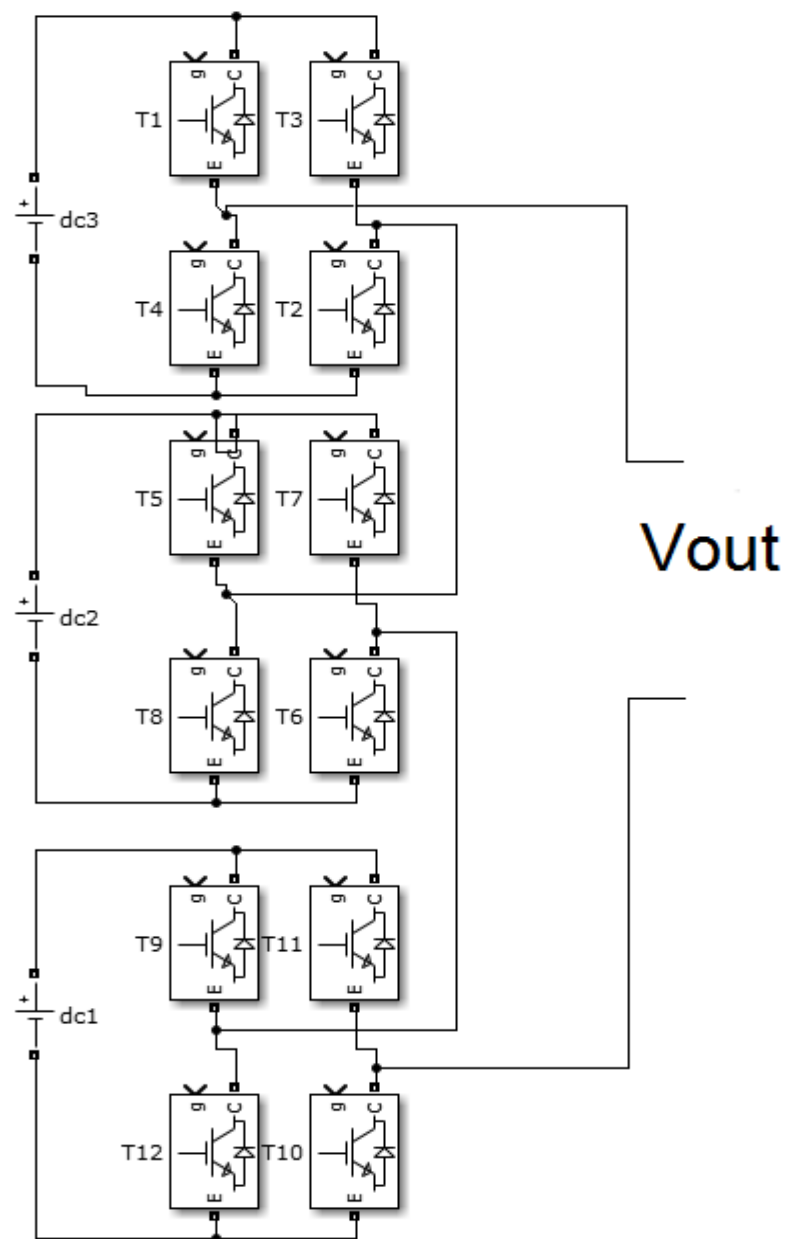


Figure (4.5): 27 Level H-bridge inverter with three separate DC source.

By controlling the switches in each H-bridge, desired or reference output waveform can be obtained.

The controller of the switches depends on the amplitude of the reference signal. The modulation technique used is amplitude modulation because it is easy and simple method. The basic principle of this method depend on the comparison between the amplitude reference signal and defended ranges to generate pulses as shown in the flowing chart.

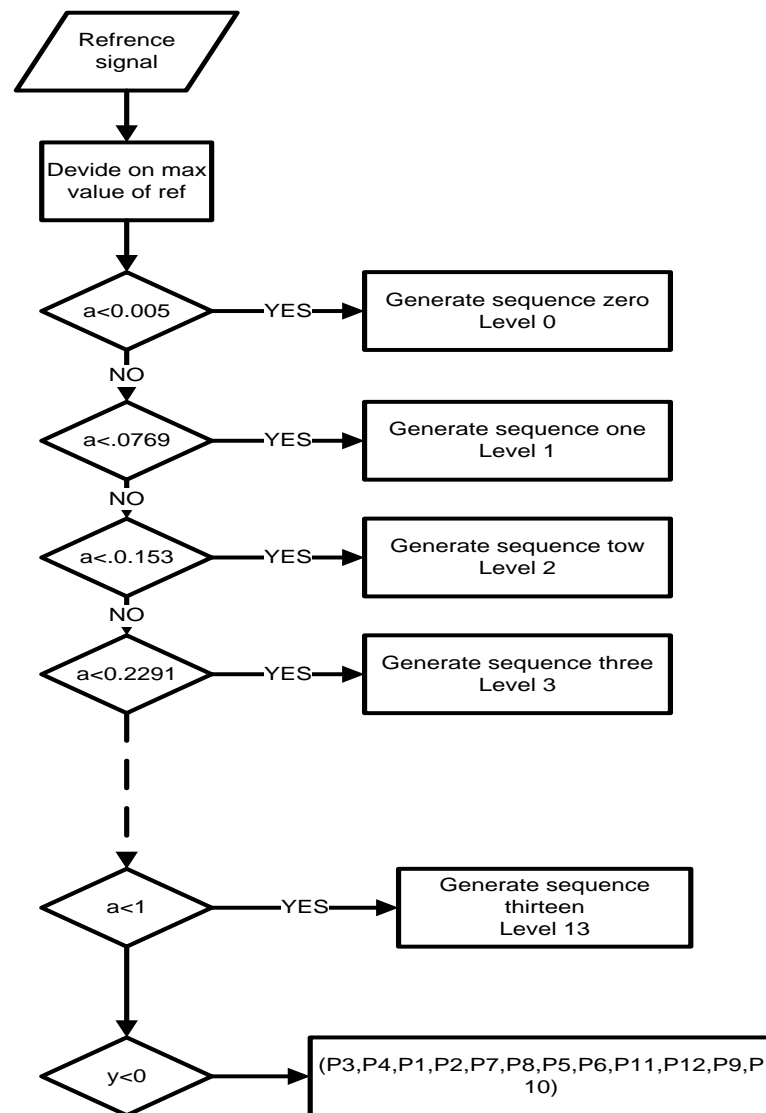


Figure (4.6): Amplitude modulation flow chart.

Where: a is the absolute value of reference signal divided on max value.

y is the value of reference signal divided on max value

The basic concept of amplitude modulation is as following steps:

- 1- Input reference signal divided on its max value.
- 2- Finding the range of each step by dividing one over (one minus number of levels) divided by tow as shown below:

$$1/([1-27]/2) = 0.0769.$$

- 3- Checking the amplitude of the input or reference signal and finding the range in which this value belongs to and generating suitable pulses to produce suitable level.

For example if the value of the signal amplitude is 0.01, it means that the output should produce level 1 because the value .01 belong to the first range (.038 to .0769).

- 4- The arrangement of the pulses which fed the switches is as following:

(P1 , P2 , P3 , P4 , P5 , P6 , P7 , P8 , P9 , P10 , P11 , P12) for positive values of reference signal and as following

(P3 , P4 , P1 , P2 , P7 , P8 , P5 , P6 , P11 , P12 , P9 , P10) for negative values of reference signal.

For example if the value of the input reference signal is .060 then the output voltage should be level one which equal 36 volt so the first DC voltage should be connected and the tow others should be disconnected.

The controller produce pulses for the switches to achieve this as following (110010101010).

The DC voltages arrangement will be as shown in the following figure

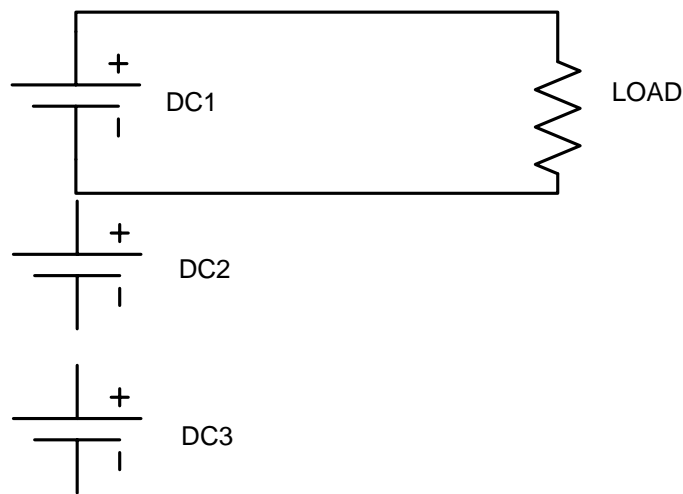


Figure (4.7): The DC voltages arrangement for level 1.

Another example, when the value of the signal amplitude equal 0.62 then the output voltage should be level 8 which equal $36 \times 8 = 288$ volt. In this case, DC3 (323V) will be connected in positive mode and DC1 (36) will be connected also but in negative mode as shown in figure 4.8

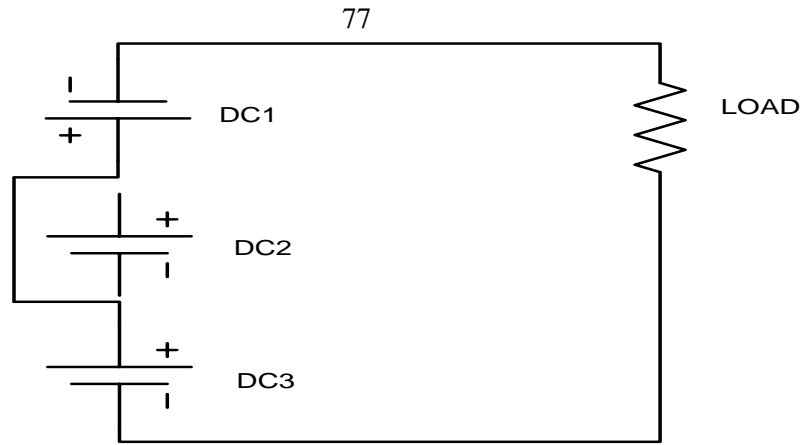


Figure (4.8): The DC voltages arrangement for level 8.

To achieve this arrangement of voltages, the controller will produce the following gate pulses (001110101110).

The output voltages of each module (cell) and the total voltage are shown in the figure (4.9).

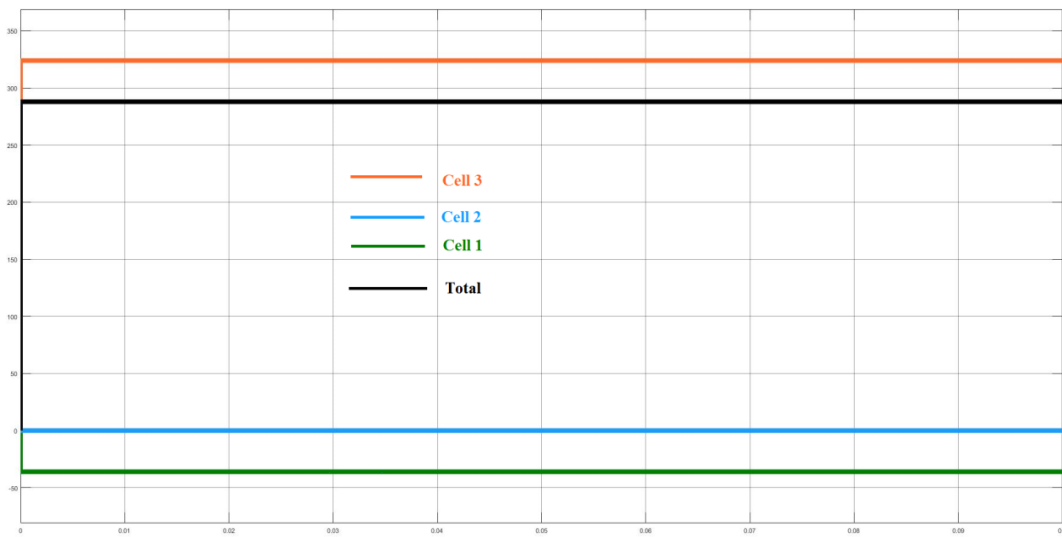


Figure (4.9): The output voltages of each cell when (001110101110) produced.

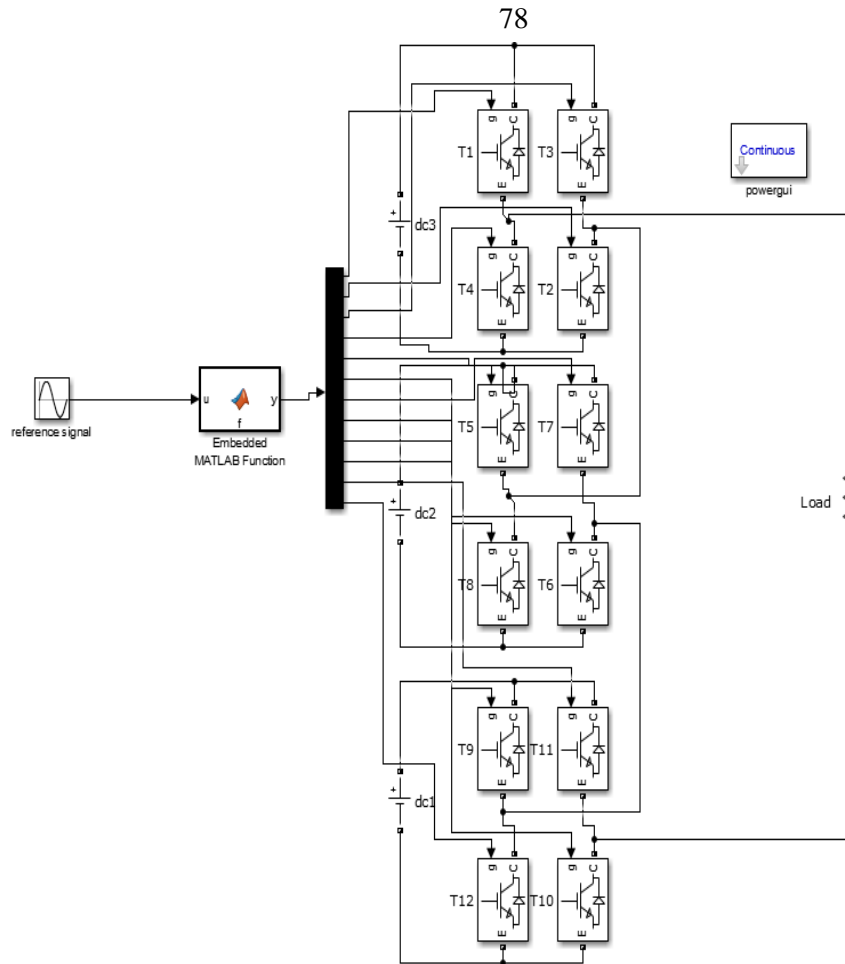


Figure (4.10): 27 level H-bridge inverter with its controller.

4.4 Results

To test the performance of the proposed H-bridge inverter, five cases are simulated by using MATLAB software.

- Case1: using two level inverter with sinusoidal input.
- Case2: using nine level H-inverter with sinusoidal input.
- Case3: using 27 level H-inverter with sinusoidal input.
- Case4: using three level H-inverter to produce reference signal needed in the thesis.

- Case5: using 27 level H-inverter to produce reference signal needed in the thesis.

4.4.1 Simulation of Tow-Level Inverter with Sinusoidal Input.

The input signal is sine wave with frequency equal 50 Hz.

Based on the modulation technique which is explained in the previous section, two pulses are generated. These pulses will feed the switches of the inverter to produce either +DC or -DC output voltage depending on the amplitude of the input voltage.

The input and the output voltages are shown in figure (4.11).

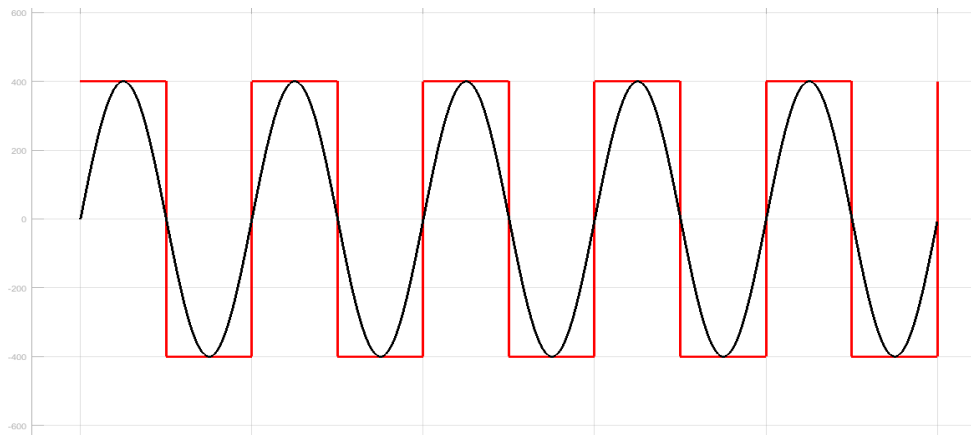


Figure (4.11): The input and output voltage signals using two level inverter.

The total harmonic distortion (THD_V) equal 48.3% (using MATLAB software to measure THD_V).

4.4.2 Simulation of Nine-Level Cascade Inverter with Sinusoidal Input.

The input signal is sine wave with frequency equal 50 Hz.

Based on the modulation technique which is explained in the previous section, twelve pulses are generated. These pulses will feed the switches in one phase leg of a nine level inverter. Similarly the remaining two phases are fed by the same pulses generated, but changing phase shifting angle of modulating signal by 120 degrees to produce three phase system.

The input and the output voltage signals are shown in the figure (4.12).

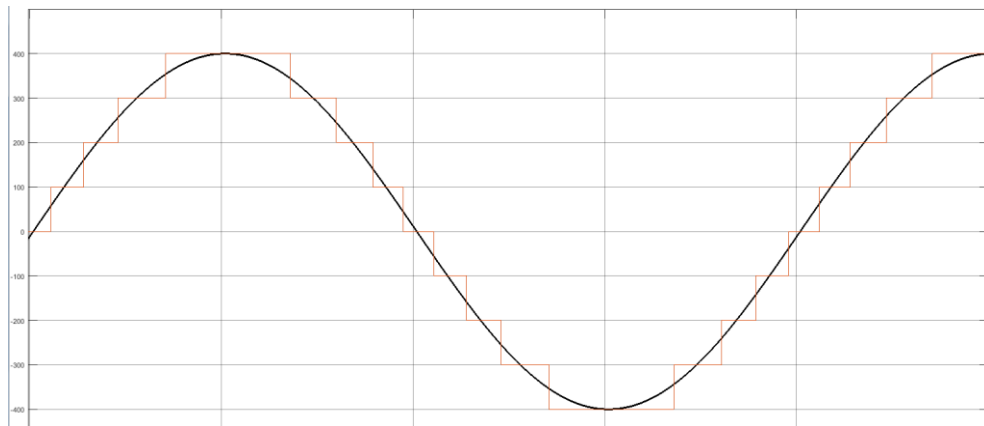


Figure (4.12): The input and output voltages using nine level H-bridge inverter.

The total harmonic distortion (THD_V) equal 9.38%.

4.4.3 Simulation of 27 Level Cascade Inverter.

The same parameters for the input signal are used when using the 27 level inverter.

The input and the output voltage signals are shown in figure (4.13)

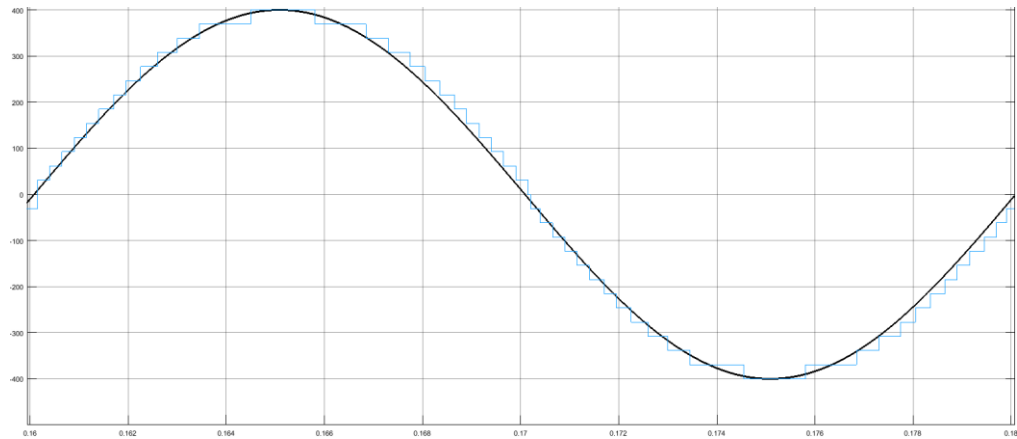


Figure (4.13): The input and output voltage using 27 level H-bridge inverter.

The THD_V when using 27 level inverter equals 5.05%.

By comparing the results obtained from three types of inverters, the following notices can be observed:

- 1- The output voltage when using 27 level inverter is closer to sinusoidal or reference signal.
- 2- The total harmonic distortion when using 27 level inverter is lower.
- 3- The 27 level inverter is more suitable to be used in the project to minimize the THD for the source current.
- 4- Two level inverter have large THD.

4.4.4 Simulation of Three Levels Inverter.

A three level inverter is used to produce the reference signal which is generated by the controller mentioned in chapter three.

The output source current when using three level inverter is shown in figure(4.14):

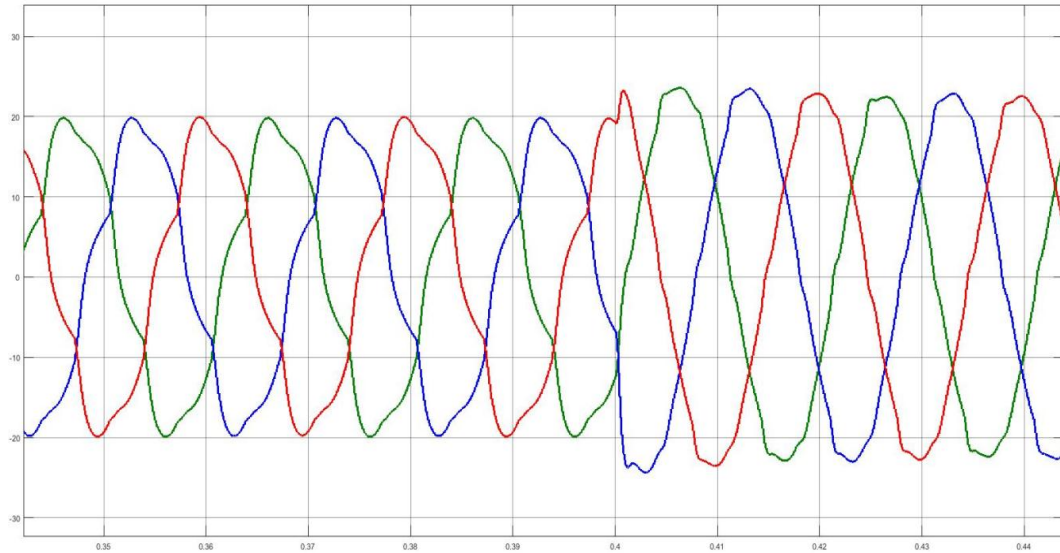


Figure (4.14): Output source current after using three level inverter.

At time zero, the system works without connecting the active filter which consists of three level inverter but at time 0.4 second, the inverter is connected and starts to compensate the harmonics so the total harmonic distortion (THD_I) for the supply current decreases to 6.32% which needs to be decreased more (according to IEEE-STD-519-2014) [44].

4.4.5 Simulation of 27 Level Inverter.

27 level inverter is used instead of three level inverter and it is connected at time 0.4 second to the system and the THD_I becomes 3.9% which is accepted (according to IEEE-STD-519-2014) [44].

The following output current is obtained after and before connecting the new inverter.

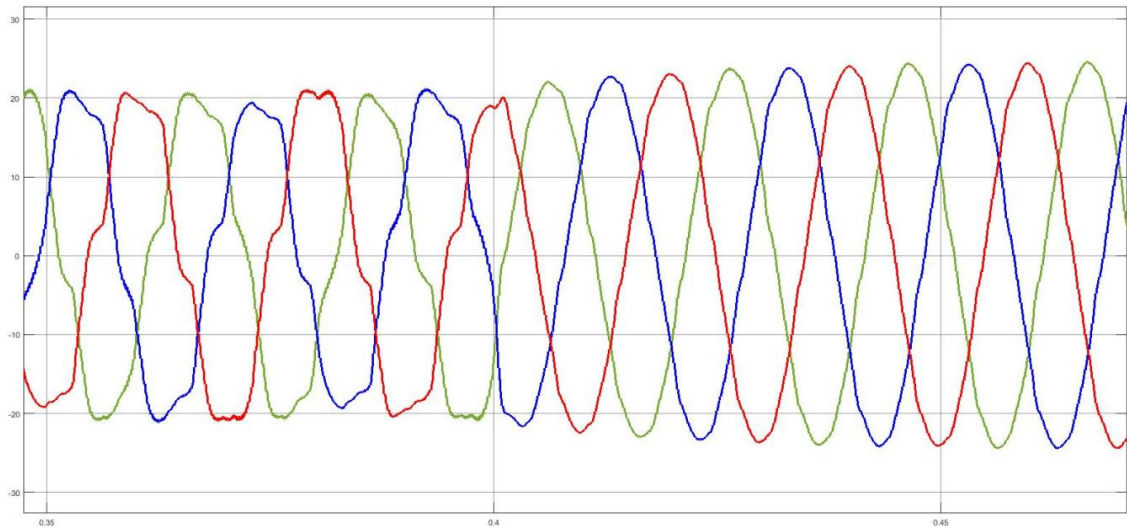


Figure (4.15): Output source current before and after using 27 level inverter.

From figure (4.15), it is clear that the output current is more accurate and the THD_I is less in comparison with three level inverter. So when the number of levels increases, it means better performance.

Table 4.3 shows a comparison between the results obtained from the five cases.

Table 4.3 : Comparison between the results obtained from the five cases.

Case	Input signal	Number of levels	THD
Case 1	Sine (50 Hz)	2	48.3%
Case 2	Sine (50 Hz)	9	9.38%
Case 3	Sine (50 Hz)	27	5.05%
Case 4	Reference signal (output of controller)	3	6.32%
Case 5	Reference signal (output of controller)	27	3.9%

Chapter Five

Fault Tolerant Techniques for the H-Bridge Inverter.

5. Fault Tolerant Techniques for the H-bridge Inverter.

5.1 Introduction

Recently , the voltage source inverters (VSI) are used widely specially in the industrial applications ,such as railway traction , aeronautics and robotics, and other fields like distributed generations which connected to the power systems ,some of these distributed generations use inverters which depend on the power switches like insulated-gate bipolar transistors (IGBTs) because of their fast switching ,high efficiency and they can handle short-circuit currents for considerable period of time [35]. Although of its advantages, the inverter can be affected by abnormal conditions which can damage the power switches causing faults in the system. Three main types of failure of power switches operation can occur such as the intermittent gatemisfiring fault, open circuit fault, and the short-circuit fault [35]. So, to achieve the reliability and availability of the inverters, some fault-tolerance techniques have to be applied to ensure that the inverter still can operate under fault conditions.

In this thesis, an open circuit fault for one phase of the inverter is considered (as shown in figure 5.1) by assuming one leg is disconnected.

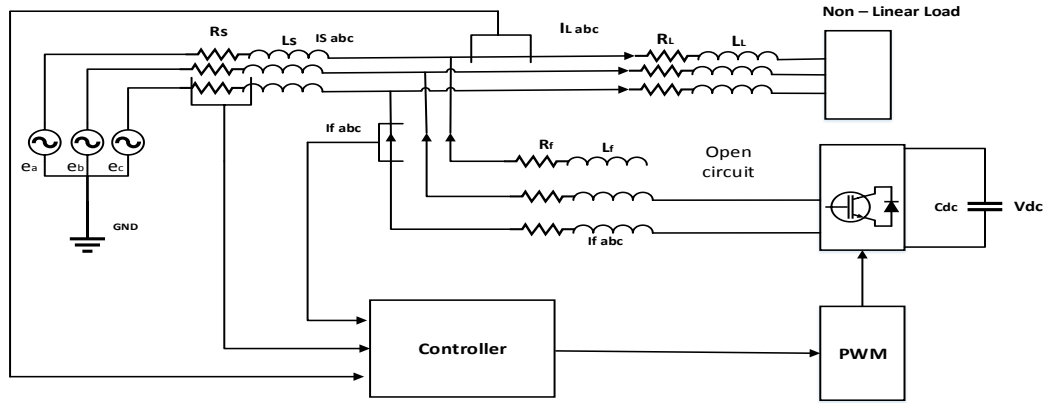


Figure (5.1): Diagram of the system with open circuit fault.

After applying this assumption on the designed system, the total harmonic distortion (THD_I) for the faulted phase (c) becomes about 42% which is very large (according to IEEE-STD-519-2014) and the output source current signal becomes destroyed as shown in figure (5.2)

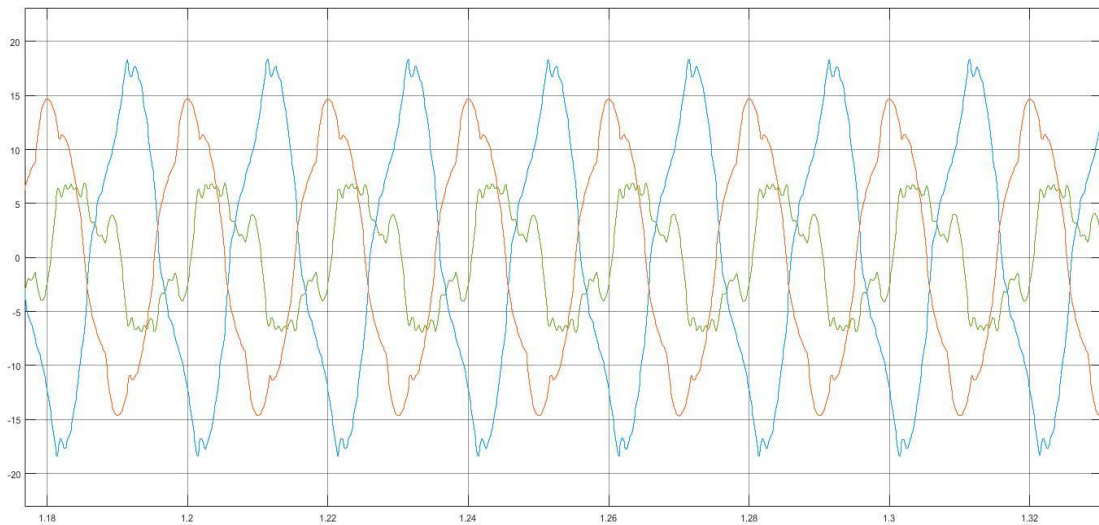


Figure (5.2): Output source current during open circuit fault.

5.2 Fault-Tolerant Two-Level Inverter Techniques

Historically, fault tolerance techniques in energy conversion systems have been used for motor drives that suffer from many types of external faults especially external phase-loss (PL) fault. At first, the fault tolerance techniques was applied on the Y-three phase motor drive by adding auxiliary fourth leg to the conventional two level inverter topology, and the neutral point of stator windings of the motor is connected to the added fourth leg as shown in figure 5.3 [36].

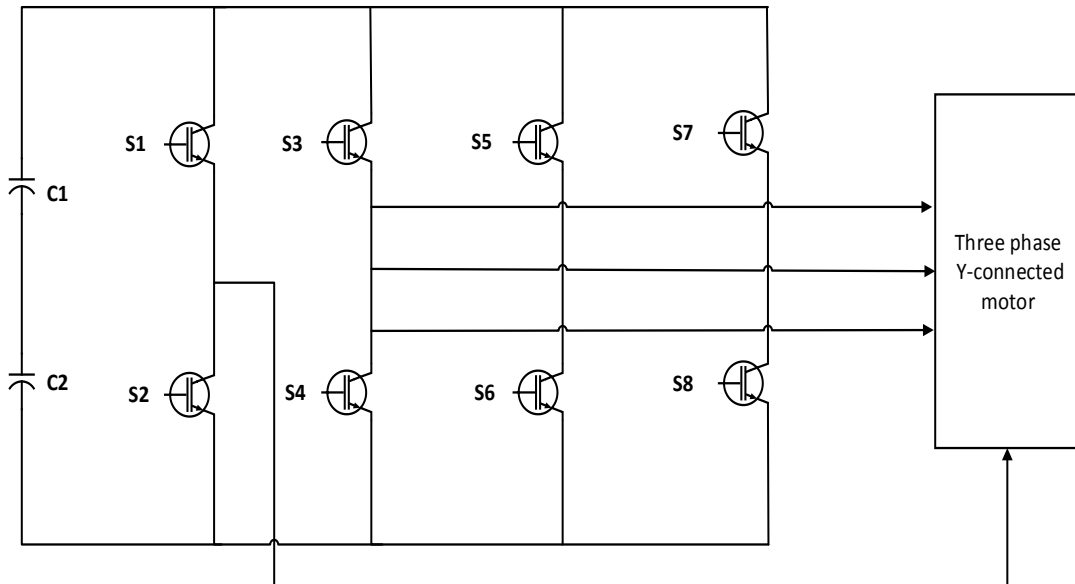


Figure (5.3): Two-level three-phase inverter with fourth leg for fault tolerance [38].

Another solution is to consider the DC-bus capacitor branch as the fourth leg [36]. The fourth leg enables the inverter to work under fault condition and continue to supply the motor as normal operation with open circuit phase and two running phases.

Another technique is to supply a three-phase load from two phases with 60° phase shift, this technique was proposed in 1982 [37]. The idea is to make the inverter have the ability to inject line currents such that the phase shift angle about 60° with respect to each other when the faulted phase is isolated, this make the rotating MMF with only forward component, but the value of MMF in case of fault condition is about $1/\sqrt{3}$ of the magnitude in case of normal operation, so the output power to the motor will decrease about $1/\sqrt{3}$ of its rated power [37]. Thus the value of remaining two currents must be increased by $\sqrt{3}$ factor if rated power is needed.

The forth leg technique can be used also when there is an internal fault in the inverter in addition to the phase loss (PL) fault. This can be achieved by isolating faulty leg by using fast-acting fuses which have the ability to disconnect the circuit before damaging the power switches (high response).

This fault tolerant technique can tolerate the following faults:

- 1- Switch open circuit (SOC).
- 2- Switch short circuit.
- 3- Leg open circuit.
- 4- Leg short circuit.

There are many topologies for this tolerant technique as shown in figure (5.4) and figure (5.5)

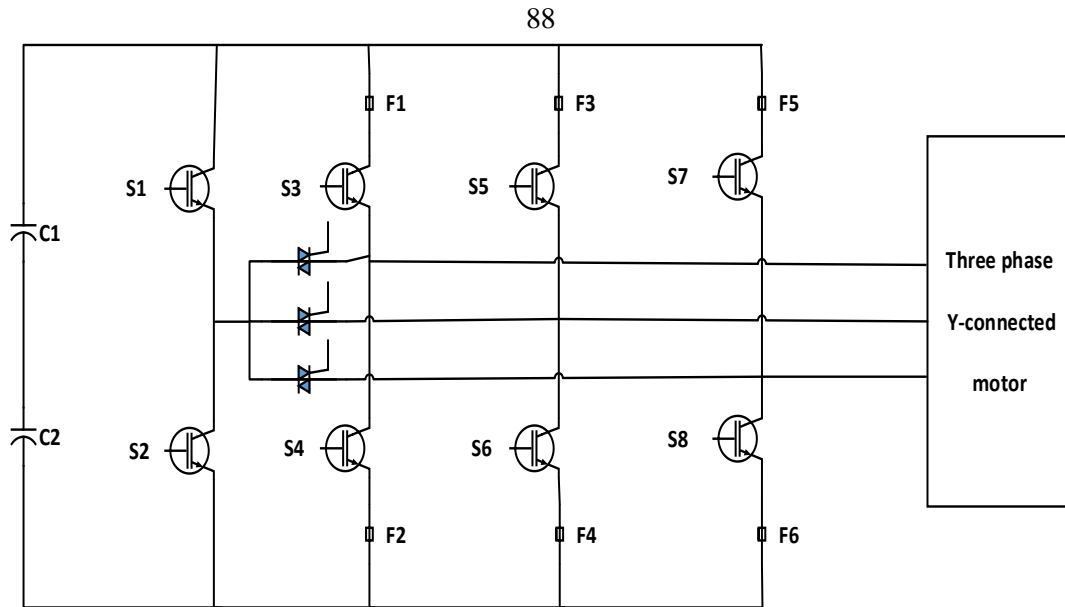


Figure (5.4): Fault-tolerant topology for two level four-leg inverter.

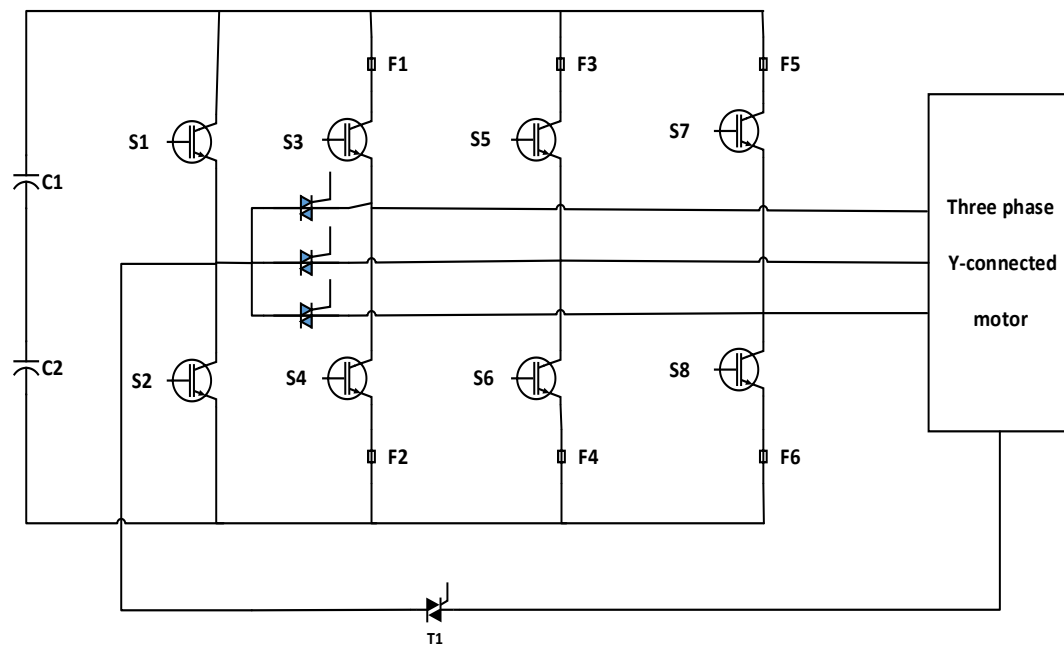


Figure (5.5): Fault-tolerant topology for two level four-leg neutral-point-connected inverter.

The topology shown in figure (5.4) can tolerate short and open-circuit switch faults. It uses fourth leg which is connected to the other three legs through group of triacs. In normal or healthy conditions, the inverter

operates with three main legs and the triacs are off. When the fault occurs, the faulty leg is disconnected and isolated by using fast-acting fuses and the corresponding terminal of the load is connected to the midpoint of the fourth leg by firing triac which connected to it.

The other topology shown in figure (5.5) can tolerate both phase loss (PL) and switch faults except a leg short-circuit fault [38]. The motor neutral point is connected to the midpoint of the fourth leg to tolerate the PL faults. When the fault occurs, the triacs isolate the faulty leg and the fourth leg is activated by turning on the corresponding triac.

To tolerate a short-circuit leg by using this topology, a set of thyristors and capacitors should be added as shown in figure (5.6).

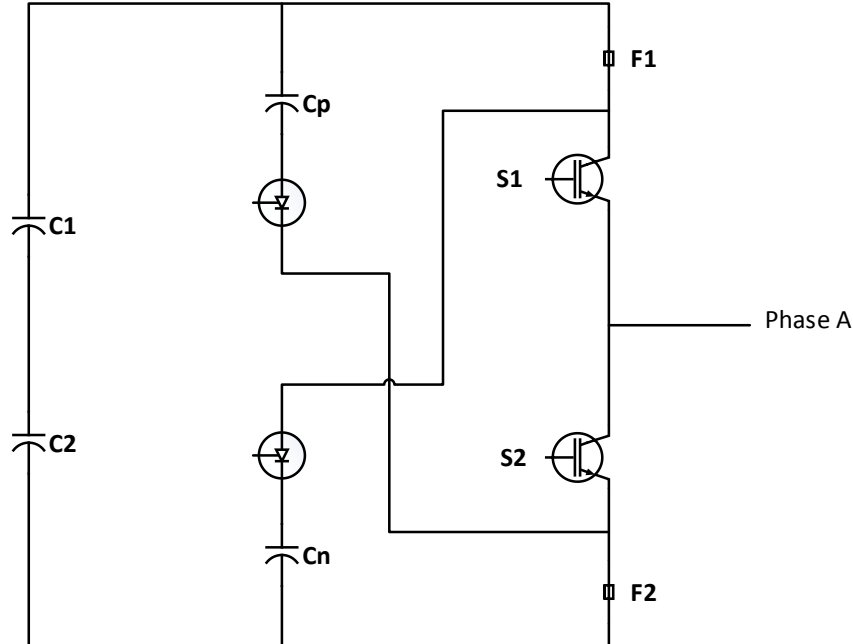


Figure (5.6): Leg A with isolation capability.

The above schematic of leg have the ability to isolate the short circuit fault of the two switches .If the fault in the lower or upper switch occur , the associated thyristor is activated to open the fuse and isolate faulty switch. The value of the added capacitors should be chosen depending on the thyristor current and have the ability to open fuse quickly [39].

5.3 Fault-Tolerant Multilevel Inverters

The multilevel inverter consists of large numbers of semiconductor power switches so, this type suffer from internal faults more than two level inverters [40]. Fault tolerance for multilevel inverters usually achieved by isolating the faulty device or module and reconfiguring the switching pattern for the other modules to new normal condition [41]. Sometimes, no need for the fourth auxiliary leg to tolerate the faults which is mostly used as a solution in two level inverters. Many fault tolerant topologies are used for multilevel inverters, including all types such as flying capacitor, cascaded H-bridge and neutral-point clamped inverters.

Fundamental phase-shift compensation (FPSC) is an example of fault tolerant techniques; this technique can tolerate both short circuit and open circuit faults by isolating the faulty device or module using bypass contactor as shown in figure (5.7).

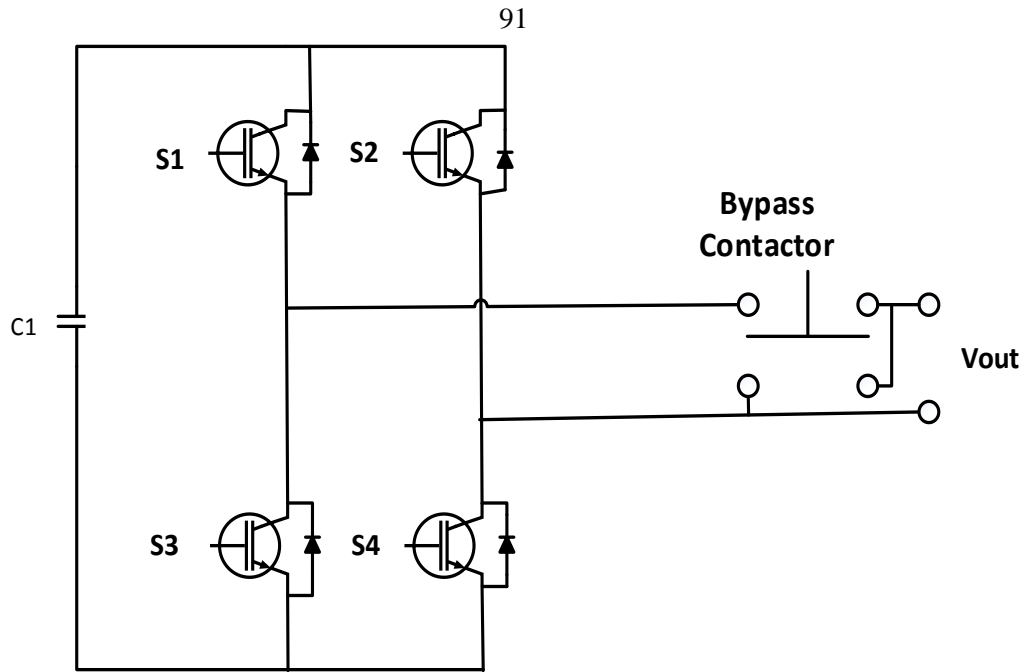


Figure (5.7): Module with bypass contactor.

The line to line voltages output before and after fault for cascaded multilevel inverter remain balanced. During fault; new calculations for the angles between phases are needed to keep the line to line voltages balanced. This technique is very effective and simple [43]. Sometimes, the new angles can't be calculated because the nonlinear equations have no solutions and the inverter neutral point outside of the line-line voltage triangle or the summation of the two healthy legs less than or equal to the third leg. So, a new technique is used which is called modified FPSC technique [42].

5.4 Control Strategy for the Open Circuit Fault Adopted in the Project.

The strategy depends on adding auxiliary fourth leg to the inverter and connecting it to the neutral point of the load as shown in figure (5.8)

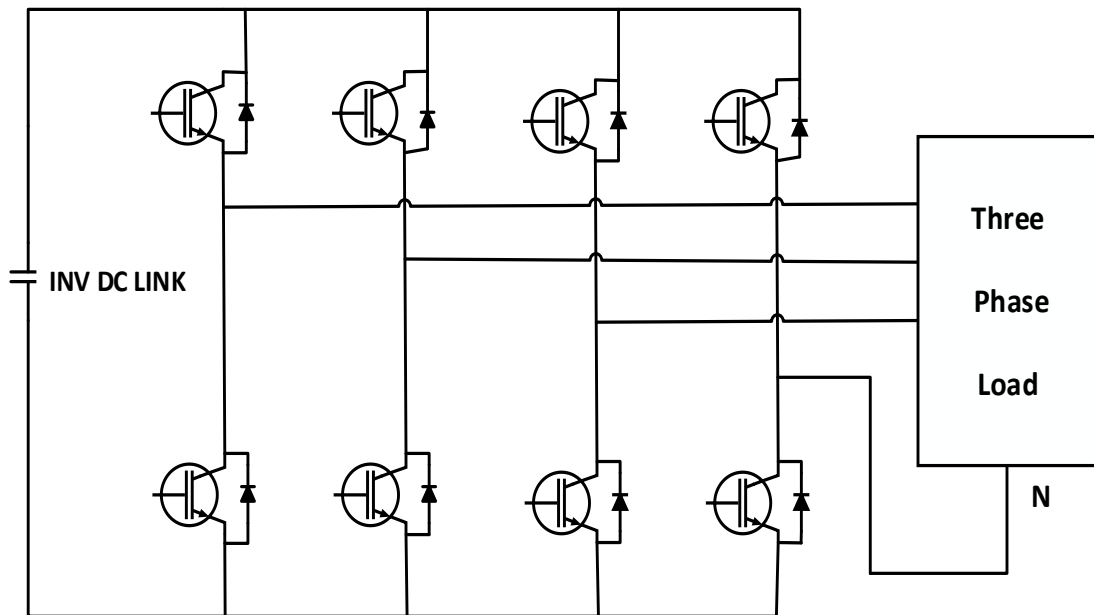


Figure (5.8): Fault tolerant scheme for one leg open circuit.

The added fourth leg is to provide the ability for the inverter to tolerate an open phase fault. This leg is disconnected during healthy operating conditions through special switches which mean no connection between supply and neutral point. When an open circuit fault occurs, the faulty leg will be disconnected through corresponding switches and the other switches which connecting the fourth leg will be activated to control the voltage at neutral point.

To keep the performance of the inverter when an open circuit fault occur as in healthy mode, the control strategy used should be modified to control the remaining two healthy phases as following steps [43]:

- The reference voltage of the faulty phase is set to zero, for example if phase c become faulty then V_{c_ref} and I_{c_inv} should be zero.
- Activating the switches which connect the fourth leg of the inverter to the neutral point of the load.
- The current passing through the fourth leg is the sum of the two remaining currents which can be circulated.

After applying these steps to the control strategy used in chapter two,

a new control strategy is obtained as shown in figure (5.9)

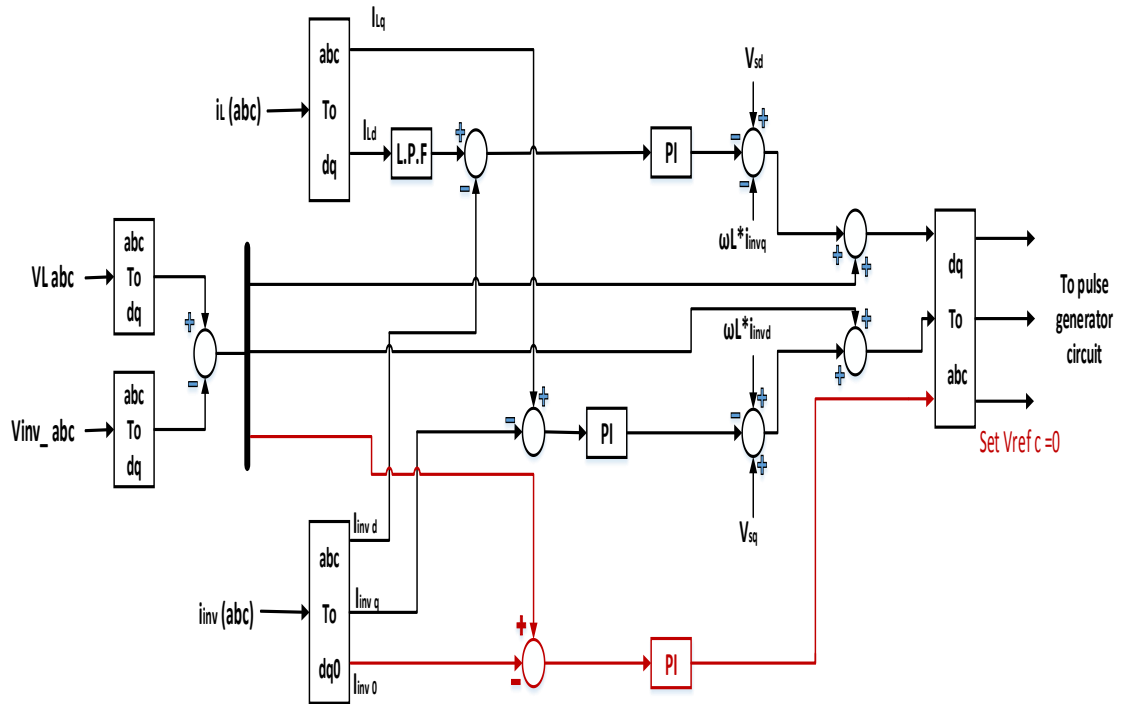


Figure (5.9): Control strategy scheme for open circuit fault.

This control strategy was applied to control the motor drive during an open circuit fault and to control speed, it was very effective during open circuit fault [43]. In this work, the same strategy is applied to the active filter during an open circuit fault.

The control strategy used to control the filter is changed to the new strategy and the output source current before and after open circuit fault is shown in figure (5.10) and figure (5.11).

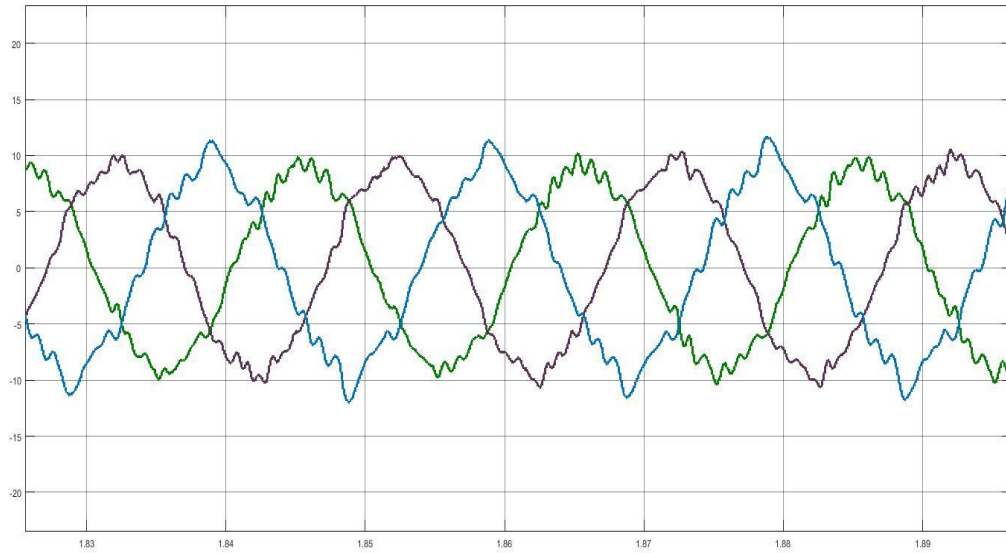


Figure (5.10): Output current after applying new control strategy for open circuit fault.

The total harmonic distortion becomes 8.4% which is acceptable in faulty condition and the distorted output source current signal becomes better and accepted as shown in figure (5.11).

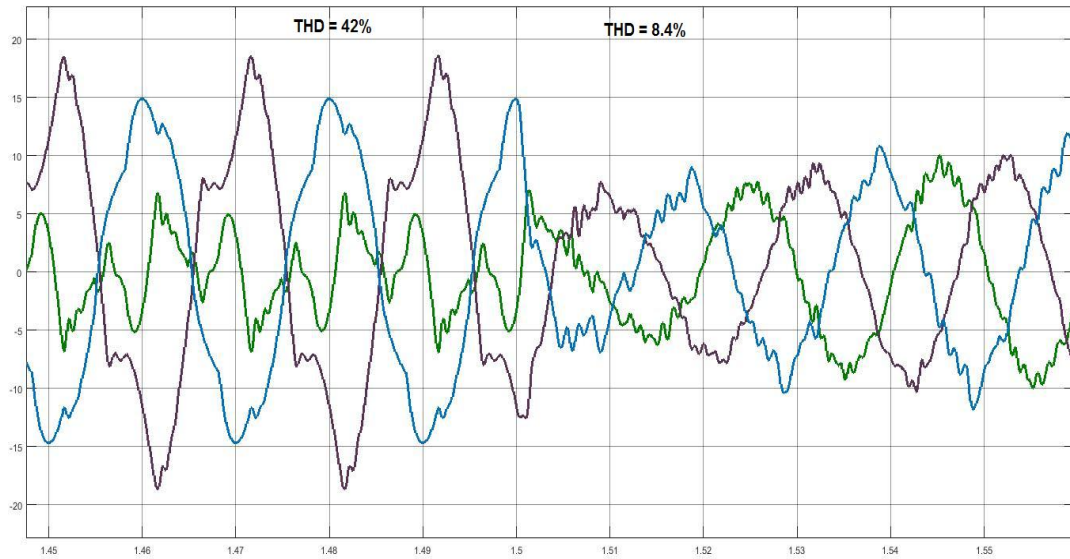


Figure (5.11): Output source current before and after applying new control topology for open circuit fault.

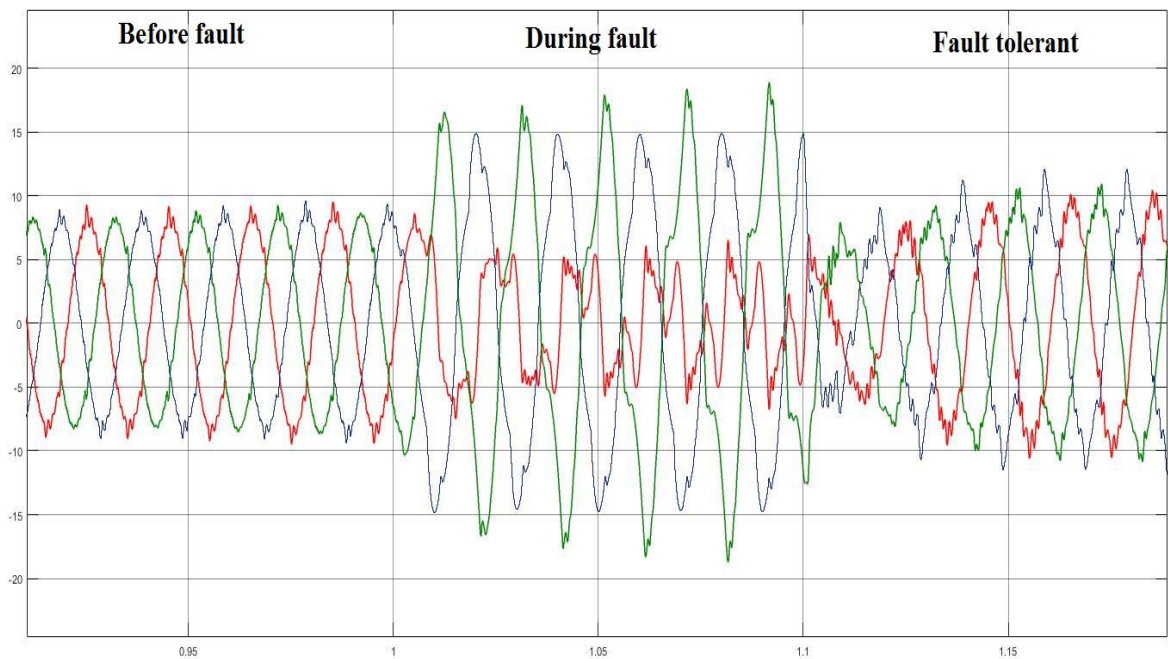


Figure (5.12): Output source current before, during and fault tolerant stages.

From the obtained results, it is seen that the inverter have the ability to work under faulty condition (open circuit fault) because the THD obtained is improved.

Conclusions

An active power filter has been designed with many tasks as following:

- It has the ability to mitigate harmonics.
- Compensate reactive power and improve power factor
- Inject real power.
- Have the ability to tolerate an open circuit fault and continue to work under faulty condition without affecting the power system.

This work consists of many stages; first stage is designing the controller for the power filter to mitigating the harmonics and compensate the reactive power. The controller is tested by using MATLAB software and connected to controlled voltage sources. The current source THD was 13.9% and becomes 1.9% after connecting the power filter at time 0.4s. The power factor also becomes around 1 which means that the reactive power produced by the source becomes around zero. The second stage is using three level inverter instead of controlled voltage sources, the THD for the source current becomes 6.39% and the power factor around 0.92 which means that the used inverter have to be modified to get better results. After that, 27 level inverter is used instead of three level inverter so the THD become 3.9% and the power factor become 0.99. When the levels of the inverter increase, the THD become better and the obtained signal becomes more accurate and similar to the reference signal. Amplitude modulation technique is used because it is simple and easy specially when using high

level inverter. One important task that is added to the designed filter is a fault tolerance capability which enable the filter to continue to work under faulty condition (open circuit fault). This task achieved by adopting new technique that was used in motor drive during open circuit fault . This technique applied in this project and the result is good because during fault the THD was 42% and becomes 8.4% after activating this technique at time 1.5s.

The filter is very important element in the power system to improve the power quality and to avoid the effects of increasing use of nonlinear loads.

The designed filter can not only improving power quality but also can inject real power and can also tolerate fault at the same time.

Table 7.1 shows the obtained results (for THD_I) for all stages.

Table 7.1: Results for all stages.

Case	THD_I (source current)
System without connecting active filter	13.9%
Active filter with controlled voltage source	1.9%
Active filter with three level inverter	6.32%
Active filter with 27 level inverter	3.9%
Active filter with one leg open circuit fault (phase c)	42% (for phase c)
Active filter with fault tolerant technique (during fault)	8.4%

References

- [1] M. Rawa, D. Thomas and M. Sumner, "**Simulation of non-linear loads for harmonic studies**", IEEE/ EPQU Lisbon-Portugal, pp.1-6, Oct. 2011.
- [2] R. Henderson, P. Rose, "**Harmonics: The effects on power quality and transformers**", IEEE Trans. Ind. Appl., vol. 30, pp. 528-532, May/June 1994.
- [3] A. Ganiyu, O. Olaluwoye, "*Effect of Reactive Power Flow on Transmission Efficiency and Power Factor*", **International Journal of Recent Scientific Research**, Vol. 6, Issue, 7, pp.5249-5253, July, 2015.
- [4] A. Patil and C.P Vijay, "*Harmonic metigation using Passive Filter*", **International Journal of Engineering Trends and Technology (IJETT)**, Volume-45-Number2, March 2017.
- [5] A. R. Dekka, A. R. Beig and M. Poshtan, "**Comparison of Passive and Active Power Filters in Oil Drilling Rigs**", IEEE/EPQU conference, Lisbin-Portugal, pp. 1-6, June, 2011.
- [6] S. Bhattacharya, D. Divan, "**Active filter solutions for utility interface of industrial loads**", Proceedings of the International Conference on Power Electronics, Drives and Energy Systems for Industrial Growth, January 8-11, 1996.

- [7] B. R. Lin, K. T. Yang, W. Kuan, "**Hybrid Active Power Filter for power quality compensation**", 2005 International Conference on Power Electronics and Drives Systems, vol. 2, pp. 949-954, Nov 2005.
- [8] S. C. Prasad, D. K. Khatod, "*A Review on Selection and Usage of Modern Active Power Filter*", **International Journal of Engineering Trends and Technology (IJETT)**, Volume 20, Number 2, Feb 2015.
- [9] B. Singh, K. Al-Haddad, A. Chandra, "**A Review of active filters for power quality improvement**" IEEE Trans. Ind. Electron., vol. 46, No. 5, pp. 960-971, Oct. 1999.
- [10] M. Routimo, M. Salo, H. Tuusa, "**Comparison of voltage-source and current-source shunt active power filters**", IEEE Transactions on Power Electronics, vol. 22, no. 2, pp. 636-643, Mar. 2007.
- [11] K. Ragavan, "*Reference current extraction through sliding DFT assisted single phase p-q theory for shunt active power filter*", **International Journal of Emerging Electric Power Systems (IJEPS)**, May. 2013.
- [12] J. Afonso, M. Freitas, J. Martins, "**P-q theory power components calculations**", Proc. IEEE Int. Symp. Ind. Electron., pp. 385-390, Jun. 2003.
- [13] H. Akagi, "**New trends in active filters for power conditioning**", IEEE Trans. Ind. Appl., vol. 32, no. 6, pp. 1312-1322, Nov./Dec. 1996.

- [14] S. Mikkili, A. K. Panda, "**Instantaneous Active and Reactive Power and Current Strategies for Current harmonics cancellation in 3-ph 4wire SHAF With both PI and Fuzzy Controllers**", Energy and Power Engineering, vol. 3, no. 03, 2011.
- [15] V. Soares, P. Verdelho, G. D. Marques, "**An instantaneous active and reactive current component method for active filters**", IEEE Trans. on Power Electronics, vol. 15, no. 4, pp. 660-669, 2000.
- [16] T. Noguchi, H. Tomiki, S. Kondo, I. Takahashi, "**Direct power control of PWM converter without power-source voltage sensors**", IEEE Trans. Ind. Applicat., vol. 34, pp. 473-479, May/June 1998.
- [17] F. Briz, M. W. Degner, R. D. Lorenz, "**Analysis and design of current regulators using complex vectors**", IEEE Trans. Ind. Appl., vol. 36, no. 3, pp. 817-825, May/Jun. 2000.
- [18] J. Chelladurai, G. S. Ilango, C. Nagamani, S. Kumar. "*Investigation of various PWM techniques for shunt active filter.*" **International Journal of Electrical Systems Science and Engineering** 1, no. 2, pp. 87-93, 2008.
- [19] B. Subudhi, R. Pradhan, "**A comparative study on maximum power point tracking techniques for photovoltaic power systems**", IEEE Trans. Sustain. Energy, vol. 4, no. 1, pp. 89-98, Jan. 2013.
- [20] X. Nguyen, N. P. Minh, "**Mathematical modeling of photovoltaic cell/module/arrays with tags in Matlab/Simulink.**" **Environmental Systems Research** 4.1, 2015.

- [21] J. Sidawi¹, R. Habchi¹ , N. Abboud¹ , A. Jaafar, " **The effect of reverse current on the dark properties of photovoltaic solar modules**", Energy Procedia 6, pp. 743-749, 2011.
- [22] D. Swapnil, N. S. Jatin, S. Bharath, " **Temperature Dependent Photovoltaic (PV) Efficiency and Its Effect on PV Production in the World**", Energy Procedia 33, pp. 311-321, 2013.
- [23] N. Faysal, U. Safayet, " **Modelling of solar cell characteristics considering the effect of electrical and environmental parameters**", Energy and Technology (ICGET) 2015 3rd International Conference on, pp. 1-6, 2015.
- [24] V. Boscaino, G. Cipriani, V. Di Dio, R. Miceli, G. Capponi, " **Experimental test of the performances of a Photovoltaic Modules Model**", ICCEP 2015, pp. 523-528, 2015.
- [25] F. Zaouia, A. Titaouinea, M. Becherifb , M. Emzianec A. Abouboua, " **A combined experimental and simulation study on the effects of irradiance and temperature on photovoltaic modules**", Energy Procedia 75, pp. 373-380, 2015.
- [26] W. Zhang, M. Peng, C. Xiaoxiao, " **A review of maximum power point tracking methods for photovoltaic system.**" In Sustainable Energy Technologies (ICSET) 2016, IEEE International Conference on, pp. 230-234, 2016.

- [27] I. B. Karki, *"Effect of temperature on the IV characteristics of a polycrystalline solar cell."* **Journal of Nepal Physical Society** 3.1, pp. 35-40, 2015.
- [28] A. K. Gupta, S. Ravi, **"Review on widely-used MPPT techniques for PV applications"**, In Innovation and Challenges in Cyber Security (ICICCS-INBUSH), 2016 International Conference on, pp. 270-273. IEEE, 2016.
- [29] J. Nedumgatt, K. B. Jayakrishnan, S. Umashankar, D. Vijayakumar, D. P. Kothari, **"Perturb and Observe MPPT Algorithm for Solar PV Systems-Modeling and Simulation"**, Annual IEEE India Conference (INDICON), December 2011.
- [30] M. Buresch, **"Photovoltaic energy systems design and installation"**, New York , McGraw-Hill , 1998.
- [31] J. Rodriguez, J. S. Lai, F. Z. Peng, **"Multilevel inverters: A survey of topologies controls and applications"**, IEEE Trans. Ind. Electron., vol. 49, no. 4, pp. 724-738, Aug. 2002.
- [32] X. Zheng, L. Song, and P. Hongying. **"Study of five-level diodes-clamped inverter modulation technology based on three-harmonic injection method."** In 2nd International Conference on Electronic & Mechanical Engineering and Information Technology, pp. 1973-1976. 2012.

- [33] T. Meynard, H. Foch, "**Multi-level conversion: high voltage choppers and voltage-source inverters**", Power Electronics Specialists Conference 1992. PESC 92 Record. 23rd Annual IEEE, pp. 397-403, 1992.
- [34] R. A. Krishna, L. P. Suresh, "**A brief review on multi level inverter topologies**", Proc. 2016 Int. Conf. Circuit Power Compute. Techno, pp. 1-6, Mar. 2016.
- [35] B. Lu and S. K. Sharma, "**A literature review of IGBT fault diagnostic and protection methods for power inverter,**" IEEE Trans. Appl., vol. 45, no. 5, pp. 1770-1777, Sep./Oct. 2009.
- [36] M. B. de R. Corrêa, C. B. Jacobina, E. R. C. da Silva, and A. M. N. Lima, "**An induction motor drive system with improved fault tolerance,**" IEEE Transactions on Industry Applications, Vol. 37, No. 3, pp. 873-879, May/Jun. 2001.
- [37] H. W. Van der Broeck, J. D. Van Wyk, "**A comparative investigation of a three-phase induction machine drive with a component minimized voltage-fed inverter under different control options**", IEEE Trans. Ind. Appl., vol. IA-20, no. 2, pp. 309-320, Mar. 1984.
- [38] B. A. Welchko, T. A. Lipo, T. M. Jahns, S. E. Schulz, "**Fault tolerant three-phase AC motor drive topologies: A comparison of features cost and limitations**", IEEE Trans. Power Electron., vol. 19, no. 4, pp. 1108-1116, Jul. 2004.

- [39] S. Bolognani, M. Zordan, M. Zigliotto, " **Experimental Fault-Tolerant Control of a PMSM Drive**", IEEE Trans. On Ind. Electron. vol.47, no.5, Oct. 2000.
- [40] B. Mirafzal, "Survey of fault-tolerance techniques for three-phase voltage source inverters", IEEE Trans. Ind. Electron., vol. 61, no. 10, pp. 5192-5202, Jan. 2014.
- [41] S. Ceballos, J. Pou, I. Gabiola, J. Villate, J. Zaragoza, D. Boroyevich, "Fault-tolerant multilevel converter topology", Proc. IEEE ISIE2006, pp. 1577-1582, July 2006.
- [42] S. Khomfoi, L. M. Tolbert, "Fault diagnosis and reconfiguration for multilevel inverter drive using AI-based techniques", IEEE Trans. Ind. Electron., vol. 54, no. 6, pp. 2954-2968, Dec. 2007.
- [43] K.Saleh, and S. Mark. "*Modeling and simulation of sensorless control of four-leg inverter PMSM drives in the case of a single-phase open circuit fault.*" Turkish Journal of Electrical Engineering & Computer Sciences 24, no. 5, pp. 3807-3820, 2016.
- [44] IEEE Recommended Practice and Requirements for Harmonic Control in Electric Power Systems, pp. 1-29, Jun. 2014.
- [45] B. M. Hasaneen, A. A. Elbaset Mohammed, "Design and simulation of DC/DC boost converter", 2008 12th International Middle-East Power System Conference, pp. 335-340, 2008.

جامعة النجاح الوطنية

كلية الدراسات العليا

تصميم مرشح قدرة فعال له القدرة على توليد طاقة فعالة وغير فعالة
واستمرارية في العمل في حال حدوث أخطاء باستخدام عاكس كهربائي
متعدد المستويات وخلايا شمسية

إعداد

أمين ماضي

إشراف

د. كامل صالح

قدمت هذه الأطروحة استكمالاً لمتطلبات الحصول على درجة الماجستير في هندسة القوى
الكهربائية، بكلية الدراسات العليا، في جامعة النجاح الوطنية، نابلس - فلسطين.

2018

ب

تصميم مرشح قدرة فعال له القدرة على توليد طاقة فعالة وغير فعالة واستمرارية في العمل في حال حدوث أخطاء باستخدام عاكس كهربائي متعدد المستويات وخلايا شمسية.

إعداد

أمين ماضي

إشراف

د. كامل صالح

الملخص

إن الزيادة المطردة في استخدام الأحمال الغير خطية يؤدي إلى زيادة التشوه في نظام الطاقة. هذه التشوهات تؤثر على جودة ونوعية الطاقة وتسبب حدوث مشاكل كثيرة بالنظام مثل هبوط فرق الجهد عند نقاط الربط، زيادة الفاقد بالشبكة، ارتفاع الحرارة ببعض الأجهزة الكهربائية وفشلها بالقيام بمهامها بالشكل الجيد مثل المحولات وأنظمة الحماية وتخريب بعضها الآخر. لذلك اقترحت هذه الرسالة حلا لتلك المشاكل الناتجة عن تشوه الموجات من خلال تصميم فلتر يتمتع بالقيام بعدة مهام حيث يستطيع ضح طاقة فعالة وغير فعالة للشبكة وكذلك تقليل التشوهات بشكل كبير ولديه القدرة على مواصلة العمل في حالة وجود عطل بأحد أرجله. لقد تم اختبار هذا المرشح باستخدام برنامج الماتلاب واستطاع تقليص نسبة التشوه من 13.9% إلى 3.9% وقام بتحسين معامل القدرة ليصل إلى تقريبا 1 وهذا يؤدي إلى تقليل نسبة الفاقد في الشبكة. تم افتراض وجود عطل في إحدى أرجل المرشح وأظهرت النتائج قدرته على الاستمرار بالعمل بنتائج مقبولة حيث استطاع تخفيض نسبة التشوه من 42% إلى 8.4%.

من خلال هذه الدراسة تحققنا من أهمية وجود مرشحات بالشبكة لتحسين جودة ونوعية الطاقة وكذلك للمحافظة على المعدات الكهربائية.

